6.17
Long-lived Isotopic Tracers in Oceanography, Paleoceanography, and Ice-sheet Dynamics

S. L. Goldstein and S. R. Hemming

Columbia University, Palisades, NY, USA

6.17.1 INTRODUCTION 453
6.17.2 LONG-LIVED ISOTOPIC TRACERS AND THEIR APPLICATIONS 454
6.17.3 SYSTEMATICS OF LONG-LIVED ISOTOPE SYSTEMS IN THE EARTH 454
6.17.3.1 Early Applications to the Oceans 456
6.17.4 NEODYMUIM ISOTOPES IN THE OCEANS 458
6.17.4.1 REEs in Seawater 458
6.17.4.2 Neodymium-isotope Ratios in Seawater 459
6.17.4.3 Where does Seawater Neodymium Come From? 462
6.17.4.4 Neodymium Isotopes as Water-mass Tracers 465
6.17.4.5 The "Nd Paradox" 467
6.17.4.6 Implications of Nd Isotopes and Concentrations in Seawater 473
6.17.5 APPLICATIONS TO PALEOCLIMATE 473
6.17.5.1 Radiogenic Isotopes in Authigenic Ferromanganese Oxides 473
6.17.5.2 Long-term Time Series in Fe–Mn Crusts 475
6.17.5.3 Hf–Nd Isotope Trends in the Oceans 475
6.17.6 LONG-LIVED RADIOGENIC TRACERS AND ICE-SHEET DYNAMICS 477
6.17.6.1 Heinrich Events 477
6.17.6.2 K/Ar ages of Heinrich Event Detritus 477
6.17.6.3 Nd–Sr–Pb Isotopes in Terrigenous Sediments 477
6.17.6.4 Isotopic and Geochronologic Measurements on Individual Mineral Grains 478
6.17.6.5 Contrasting Provenance of H3 and H6 479
6.17.6.6 Summary of Geochemical Provenance Analysis of Heinrich Layers 479
6.17.6.7 Trough Mouth Fans as Archives of Major IRD Sources 479
6.17.6.8 $^{40}Ar/^{39}Ar$ Hornblende Evidence for History of the Laurentide Ice Sheet During the Last Glacial Cycle 481
6.17.7 FINAL THOUGHTS 484
ACKNOWLEDGMENTS 485
REFERENCES 485

6.17.1 INTRODUCTION

The decay products of the long-lived radioactive systems are important tools for tracing geological time and Earth processes. The main parent-daughter pairs used for studies in the Earth and Planetary sciences are Rb–Sr, Th–U–Pb, Sm–Nd, Lu–Hf, and Re–Os. Traditionally most practitioners have not focused their careers studying paleoceanography or paleoclimate, and the vast majority of investigations using these systems address issues in geochronology, igneous petrology, mantle geochemistry, and mantle and continental evolution. These tools are not currently considered as among the "conventional" tools for oceanographic, paleoceanographic, or paleoclimate studies. Nevertheless, these isotopic tracers have a long history of application as tracers

of sediment provenance and ocean circulation. Their utility for oceanographic and paleoclimate studies is becoming increasingly recognized and they can be expected to play an important role in the future.

Frank (2002) published a general review of long-lived isotopic tracers in oceanography and authigenic Fe–Mn sediments. This chapter attempts to avoid duplication of that effort, rather, it focuses on the basis for using authigenic neodymium, lead, and hafnium isotopes in oceanography and paleoceanography. In particular, it reviews in detail the currently available data on neodymium isotopes in the oceans in order to evaluate its strengths and weaknesses as an oceanographic tracer and a proxy to investigate paleocirculation. Neodymium isotope ratios are highlighted because lead isotopes in the present-day oceans are contaminated by anthropogenic input, and dissolved hafnium thus far has not been measured. This chapter only gives a cursory summary of the results of studies on Fe–Mn crusts, which were covered extensively by Frank (2002). This chapter also summarizes the application of strontium, neodymium, and lead isotopes for tracing the sources of continental detritus brought to the oceans by icebergs and implications for the history of the North Atlantic ice sheets. This subject was not covered by Frank (2002), and in this case we summarize the major results. Dissolved strontium and osmium isotopes are treated in another chapter (see Chapter 6.20).

6.17.2 LONG-LIVED ISOTOPIC TRACERS AND THEIR APPLICATIONS

Long-lived systems are those with decay rates that are slow relative to the 4.56 Gyr age of the solar system, meaning effectively that the parent element still exists in nature. Therefore, the abundances ratios of the daughter products of decay are still increasing in rocks and water, but at rates slow enough that changes in the daughter-isotope ratios are negligible over short time periods. In this sense they contrast with short-lived radioactive systems, associated, for example, with cosmogenic nuclides and the intermediate products of uranium decay. The abundance of a nuclide formed by radioactive decay is referenced to a "stable" isotope (one that is not a decay product) for the same element. All of the long-lived radioactive decay systems have high atomic masses (from 87 amu to 208 amu) thus chemical and biological mass fractionation effects are small, unlike light stable isotopes such as those of carbon and oxygen. As a result, in a marine or ice-core sample the effects of biological or chemical mass fractionation are negligible and isotope ratios are conservative tracers, reflecting the sources of the individual elements. Transport processes on the Earth's surface generally sample a variety of continental sources, therefore in most cases the daughter isotope ratios represent mixtures from the different age terrains. If the elements are dissolved, then their isotope ratios will remain constant over any travel path as long as no additions from new sources with different isotope ratios are added. For particulates, sorting of minerals or particle sizes from a single source can lead to isotopic variability. Neodymium, lead, and hafnium are relatively insoluble elements, as a result their residence times in seawater are short relative to oceanic mixing times of ~1,500 yr (Broecker and Peng, 1982), and isotope ratios may vary both geographically and with depth in the oceans. The isotopic variability underlies their utilization as water-mass tracers. Thus far, this application has been particularly successful with neodymium.

6.17.3 SYSTEMATICS OF LONG-LIVED ISOTOPE SYSTEMS IN THE EARTH

Interpretation of the first-order isotopic variability of strontium, neodymium, hafnium, and lead in the Earth is founded on understanding the bulk chemical characteristics of the silicate Earth and how its gross differentiation has affected the parents and daughters. The best understood system among those under consideration here is $^{147}Sm \rightarrow {}^{143}Nd$. Both parent and daughter elements are rare earth elements (REEs) existing solely in the +3 oxidation state in natural systems. The rare earths are refractory during nebula condensation, partitioning into solids at high temperatures, thus the Sm/Nd and $^{143}Nd/^{144}Nd$ ratios of the Earth are considered to be the same as in chondritic meteorites, and there is a consensus on their values (Table 1).

Moreover, they are chemically similar. Both display very limited solubility in water, and differences in chemical behavior are mainly associated with atomic size. Lutetium and hafnium are also refractory elements during nebula condensation, and thus their relative abundance in the Earth are chondritic, however, at the time of writing the value of the bulk Earth $^{176}Hf/^{177}Hf$ ratio and the ^{176}Lu decay constant are being debated (Table 1). Neodymium- and hafnium-isotope ratios in this paper will be expressed as parts per 10^4 deviations from the bulk Earth values, viz., as ε_{Nd} and ε_{Hf}. For example,

$$\varepsilon_{Nd} = \left[\left\{ \frac{(^{143}Nd/^{144}Nd)_{sample}}{(^{143}Nd/^{144}Nd)_{bulk\ Earth}} \right\} - 1 \right] \times 10^4$$

The bulk Earth compositions of Rb–Sr and Th–U–Pb are less well known, complicated by the

Table 1 Accepted or commonly used parameters for long-lived decay systems.

Decay system	*Parent/daughter*	*(Present day)*	*Isotope ratio*	*(Present day)*	*Refs.*
$^{147}Sm \rightarrow {}^{143}Nd$	$^{147}Sm/^{144}Nd$	0.1966	$^{143}Nd/^{144}Nd$	0.512638	1
$^{87}Rb \rightarrow {}^{87}Sr$	$^{87}Rb/^{86}Sr$	0.09	$^{87}Sr/^{86}Sr$	0.7050	2
$^{176}Lu \rightarrow {}^{176}Hf$	$^{176}Lu/^{177}Hf$	0.0332	$^{176}Hf/^{177}Hf$	0.282772	3
$^{176}Lu \rightarrow {}^{176}Hf$	$^{176}Lu/^{177}Hf$	0.0334	$^{176}Hf/^{177}Hf$	0.28283	4
				(Initial solar system)	
$^{238}U \rightarrow {}^{206}Pb$			$^{206}Pb/^{204}Pb$	9.307	5
$^{235}U \rightarrow {}^{207}Pb$			$^{207}Pb/^{204}Pb$	10.294	5
$^{232}Th \rightarrow {}^{208}Pb$			$^{208}Pb/^{204}Pb$	29.476	5
Decay constant (yr^{-1})					
$\lambda\ ^{147}Sm$	6.54×10^{-12}				6
$\lambda\ ^{87}Rb$	1.42×10^{-11}				7, 13
$\lambda\ ^{176}Lu$	1.93×10^{-11}				8
$\lambda\ ^{176}Lu$	1.865×10^{-11}				9
$\lambda\ ^{176}Lu$	1.983×10^{-11}				10
$\lambda\ ^{238}U$	1.55125×10^{-10}				11, 13
$\lambda\ ^{235}U$	9.8485×10^{-10}				11, 13
$\lambda\ ^{232}Th$	4.9475×10^{-11}				12, 13

References are as follows: 1. Jacobsen and Wasserburg (1980); 2. O'Nions *et al.* (1977), DePaolo and Wasserburg (1976b); 3. Blichert- Toft and Albare(c)de (1997); 4. Tatsumoto *et al.* (1981) as adjusted by Vervoort *et al.* (1996); 5. Tatsumoto *et al.* (1973); 6. Lugmair and Scheinin (1974); 7. Neumann and Huster (1976); 8. Sguigna *et al.* (1982); 9. Scherer *et al.* (2001); 10. Bizzarro *et al.* (2003); 11. Jaffey *et al.* (1971); 12. Le Roux and Glendenin (1963); and 13. Steiger and Jäger (1977). For Pb isotopes the initial values for the solar system are known much better than the present-day bulk Earth, and these are given. For the Lu–Hf system, both the decay constant and the bulk Earth value are currently in dispute. The isotope ratios of Nd and Hf in the text are given as deviations from the bulk Earth value in parts per 10^4.

volatility of rubidium and lead during nebular condensation combined with the variable depletion of volatile elements in the Earth. Of these systems, there is a consensus nevertheless for the Rb/Sr and $^{87}Sr/^{86}Sr$ ratios of the bulk Earth (DePaolo and Wasserburg, 1976b; O'Nions *et al.*, 1977). For the Th–U–Pb, the refractory behavior of thorium and uranium puts strong constraints on the $^{208}Pb/^{206}Pb$ of the Earth, but the Th/Pb and U/Pb ratios are not as well constrained. The coupled nature of U–Pb isotopic evolution (two elements, and two decay systems) means that systematics of closed-system evolution of the solar system is well constrained such that planetary bodies should lie on a ~4.56 Ga isochron line in $^{206}Pb/^{204}Pb$–$^{207}Pb/^{204}Pb$ space. However, balancing the bulk Earth composition to that line has been problematic. Details of these complications are beyond the scope of this contribution, however, there are extensive discussions in the literature.

Long-lived isotopes are useful tracers for paleoceanography and paleoclimate studies because they vary over the surface of the Earth and within. Variability between the continental crust and mantle is primarily a result of (i) the gross chemical differentiation of the Earth, associated with mantle melting and plate tectonics to form continental crust, and the different behaviors of the parent and daughter elements during magma formation, and (ii) the age of the continental crust. Among the systems under consideration, Rb–Sr, Sm–Nd, and Lu–Hf isotopic variability on the Earth's surface follows general expectations from melting behavior, at least in a gross sense. Rubidium, neodymium, and hafnium are more likely to enter magma than their partner elements, and as a result the continents have higher Rb/Sr and lower Sm/Nd and Lu/Hf ratios than the Earth's mantle. During the course of time this has resulted in the continents having high $^{87}Sr/^{86}Sr$ and low $^{143}Nd/^{144}Nd$ and $^{176}Hf/^{177}Hf$ ratios compared to the mantle and bulk Earth (i.e., negative ε_{Nd} and ε_{Hf} values), as illustrated by Figure 1. Mid-ocean ridge and ocean island basalts (MORB and OIB), derived from melting of the mantle, have low $^{87}Sr/^{86}Sr$ and high $^{143}Nd/^{144}Nd$ and $^{176}Hf/^{177}Hf$ ratios (positive ε_{Nd} and ε_{Hf} values). Convergent-margin volcanics have similar isotopic characteristics as oceanic basalts as long as they are not situated on old continental crust or contain large amounts of subducted sediment.

The distinction between continental- and mantle-isotope ratios increases with the age of the continental terrain. Because the age of the continental crust is geographically variable, the continents are isotopically heterogeneous on regional scales and this heterogeneity forms the basis for tracing sources and transport. As a reflection of melting behavior and continental age, isotopic variations between some of these isotope systems are systematic in continental rocks and oceanic basalts. Nd–Hf isotopes are usually positively correlated while Nd–Sr and Hf–Sr isotopes are usually negatively correlated. However, these are gross features of the decay systems

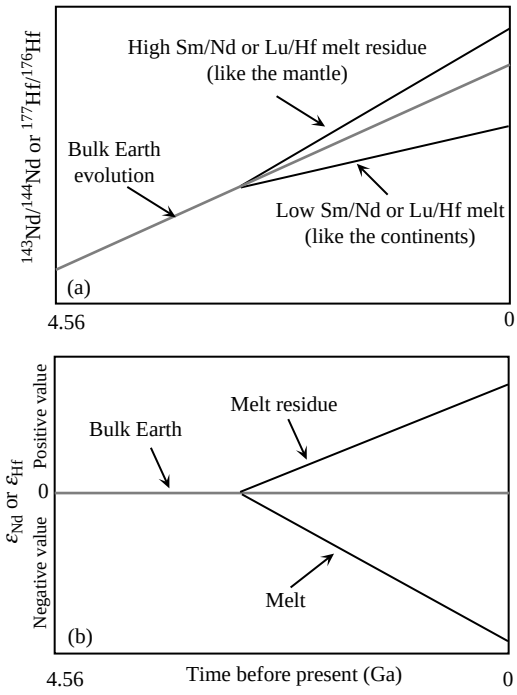

Figure 1 Systematics of Nd- and Hf-isotopic evolution in the bulk Earth, continental crust, and mantle. Daughter elements Nd and Hf are more incompatible during mantle melting (more likely to go into a partial melt of mantle rock) than Sm and Lu, respectively. As a result, the continental crust has a lower Sm/Nd and Lu/Hf ratio than the mantle, and lower Nd- and Hf-isotope ratios. Young continental crust has isotope ratios similar to the mantle, and the older the continental terrain, the lower the Nd- and Hf-isotope ratios. Rb–Sr behaves in the opposite sense, such that the parent element Rb is more incompatible than the daughter element Sr. (a) Schematic example of the evolution of Nd- and Hf-isotope ratios of a melt and the melt residue from a melting event around the middle of Earth history from a source with the composition of the bulk Earth. (b) The same scenario as in (a), but with the isotope ratios plotted as ε_{Nd} and ε_{Hf}. The "bulk Earth" value throughout geological time is defined as ε_{Nd} and $\varepsilon_{Hf} = 0$, and ε-value of a sample is the parts per 10^4 deviation from the bulk Earth value.

and there are some complicating features. For example, a significant portion of continental hafnium is located in the mineral zircon, a heavy mineral that can be separated by sedimentary processes. Therefore, in sediments where zircon has been separated by sorting, the Lu/Hf and $^{176}Hf/^{177}Hf$ ratios should be higher than expected from the crustal age. As discussed below, this appears to have important effects on the isotope ratio of dissolved hafnium in the oceans. The Rb–Sr system is more likely than neodymium and hafnium to be disturbed by weathering and metamorphism due to higher solubility of rubidium and strontium in water. In addition, minerals such as micas generally have high Rb/Sr ratios, and feldspars have lower Rb/Sr ratios; therefore, crystal sorting of a sample during transport by currents can result in significant strontium-isotopic heterogeneity of samples from the same source. These processes affecting hafnium and strontium isotopes can degrade correlations with neodymium isotopes in marine or eolian samples.

Lead-isotope ratios in continental rocks and oceanic basalts often do not display strong correlations with Nd–Sr–Hf isotope ratios, even though the melting behavior of thorium and uranium relative to lead is similar to Rb–Sr (Hofmann *et al.*, 1986). $^{206}Pb/^{204}Pb$ ratios usually show substantial overlap in oceanic basalts and continental rocks. In $^{206}Pb/^{204}Pb$–$^{207}Pb/^{204}Pb$ x–y plots, continental rocks generally fall above oceanic basalts, reflecting higher $^{207}Pb/^{204}Pb$ for a given $^{206}Pb/^{204}Pb$ ratio, a consequence of the short half-life of ^{235}U compared to ^{238}U (Table 1) coupled with a higher U/Pb ratio in the continents than the mantle over the first half of Earth history. As a result, continent-derived lead can often be distinguished from mantle-derived lead.

6.17.3.1 Early Applications to the Oceans

Investigations involving the oceans and marine sediments were among the earliest applications of long-lived radioactive systems. The first major lead isotopic study by Patterson *et al.* (1953) reported data on a Pacific manganese nodule and a red clay. This was followed by Patterson's (1956) classic work on the age of the Earth, where lead-isotope ratios of marine sediments were used to estimate the average lead-isotope composition of the Earth. Although subsequent work has shown the approach to be flawed, this work still is credited for defining the genetic link between the formation of meteorites and the Earth. Chow and Patterson's (1959) classic paper on lead-isotope ratios in manganese nodules can be considered as the work that sets the stage for all future applications of long-lived radioactive isotopes to the oceans. They wrote "the oceans serve as collecting and mixing reservoirs for leads which are derived form vast land areas, thus provide samples of leads … (reflecting) large continental segments. Lead isotopes can also be used as tracers for the study of circulation and mixing patterns of the oceans." This and their subsequent study (Chow and Patterson, 1962) outlined the geographical variability of lead in manganese nodules and pelagic clays in the oceans. They showed, for example, that different regions have characteristic lead-isotope ratios, and that they are lowest in the northwest Pacific and highest in the northeast Atlantic (Figure 2). They further

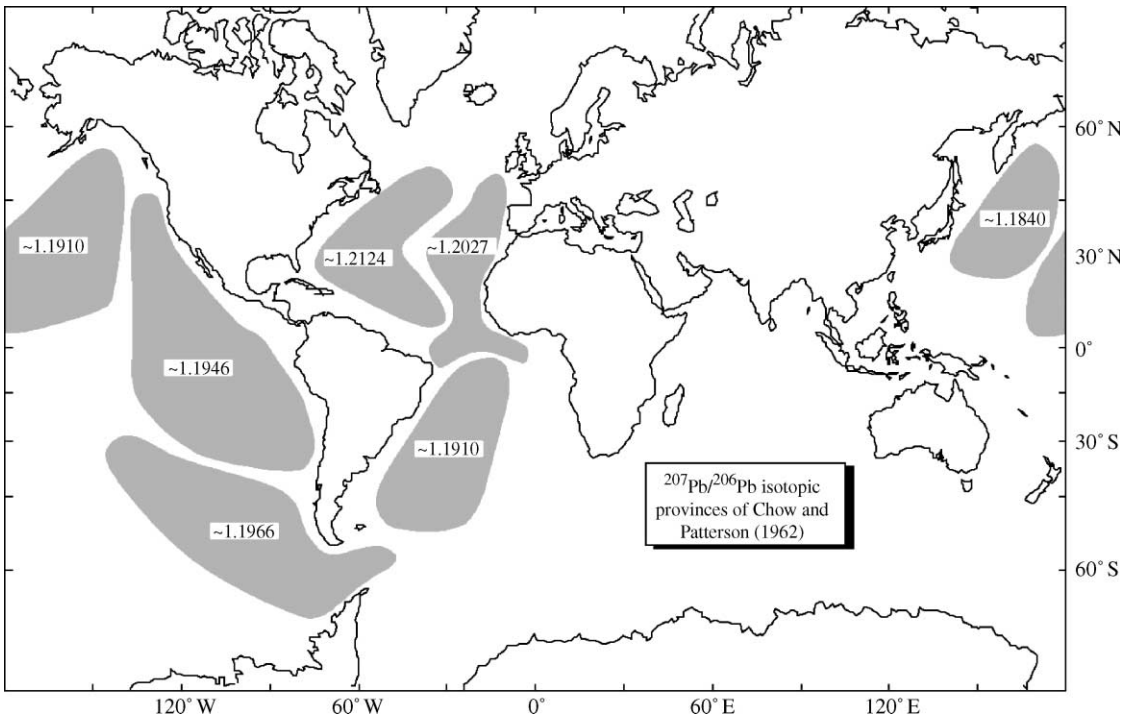

Figure 2 Marine Pb-isotopic provinces defined by Chow and Patterson (1962). The Pb-isotope ratios are given as $^{207}Pb/^{206}Pb$ ratios rather than $^{207}Pb/^{204}Pb$ and $^{206}Pb/^{204}Pb$ because of easier measurement and fractionation control. The map shows that major provinces in the oceans were defined by this early work. Among the implications is that North Atlantic Pb has an old continental provenance, defined by high $^{207}Pb/^{206}Pb$ ratios.

identified the southwest Atlantic as a province having relatively low lead-isotope ratios, like the north Pacific. They concluded that the source of marine lead is the continental crust, but without knowledge of isotopic compositions of mantle lead. Nearly a decade later, Reynolds and Dasch (1971) and Dasch *et al*. (1971) confirmed a continental source for the lead in manganese nodules and clays far from ocean ridges, but showed that manganese-rich metalliferous sediments deposited near mid-ocean ridges contain mantle-derived lead, extracted by hydrothermal processes near ridges.

The first neodymium-isotopic analyses aimed at characterizing the oceans closely followed the initial development of neodymium isotopes as a chronometer and tracer (Richard *et al*., 1976; DePaolo and Wasserburg, 1976a; O'Nions *et al*., 1977). O'Nions *et al*. (1978) was the first to report neodymium (along with lead and strontium) isotopes in manganese nodules and hydrothermal sediments. They confirmed the distinction between continental and mantle provenances of lead in hydrogenous and hydrothermal manganese sediments, respectively. Consistent with the previous studies, they found that strontium in these deposits is derived from seawater. All of the neodymium-isotope ratios in their samples from the Pacific were similar and lower than the bulk Earth value ($\varepsilon_{Nd} = -1.5$ to -4.3). They concluded correctly that neodymium in the oceans is mainly derived from the continents, and incorrectly that neodymium-isotope ratios in the oceans are like strontium isotopes in the sense that they are globally well-mixed and display this restricted range. In order to reach this conclusion they ignored a sample from the Indian Ocean having high strontium-isotope ratios and a lower, even more continent-like neodymium-isotope ratio of $\varepsilon_{Nd} = -8.5$.

The conclusion of O'Nions *et al*. (1978) that neodymium is relatively well mixed in the oceans was soon shown to be incorrect by studies of Fe–Mn sediments (Piepgras *et al*., 1979; Goldstein and O'Nions, 1981). These studies showed that the Pacific, Indian, and Atlantic oceans have distinct and characteristic neodymium-isotopic signatures. The North Atlantic has the lowest (old continent-like) values ($\varepsilon_{Nd} = -10$ to -14), the Pacific the highest ($\varepsilon_{Nd} = 0$ to -5), and the Indian is intermediate ($\varepsilon_{Nd} = -7$ to -10). The data, in addition, indicated some systematic geographic variability within ocean provinces. For example, the lowest values in the Atlantic were found in the far north, and some western Indian Ocean samples from locations near southern Africa had Atlantic-type values. In the Pacific, the highest values were found

in hydrothermal crusts or in the far northwest. The inter-ocean differences were attributed to the variability in the age of the surrounding continental crust, or significant contributions of volcanism-derived neodymium in the Pacific. During the period 1978–1981 two additional Pacific manganese nodule-analyses were published by Elderfield *et al.* (1981). Goldstein and O'Nions (1981) also showed that neodymium-isotope ratios can be distinguished in the leachable (precipitated) component of sediments and the solid-clay residue. The first direct measurements on Atlantic and Pacific seawater by Piepgras and Wasserburg (1980) showed substantial vertical variability, and general agreement with the Fe–Mn nodule and crust data for waters at similar depths. In addition, they suggested that North Atlantic Deep Water may have a distinct neodymium-isotopic signature, and that neodymium isotopes may have significant applications to paleoceanography.

In contrast to the application of lead and neodymium isotopes to the oceans, the first hafnium-isotopic study was not published until 1986. White *et al.* (1986) showed that six manganese nodules from the Atlantic, Indian, and Pacific oceans have a restricted range of hafnium-isotope ratios, with positive ε_{Hf} values (+0.4 to +0.9). Thus, hafnium isotopes neither show the distinct continental signature observed for marine neodymium-isotope ratios, nor the large variability of neodymium-isotope ratios in the different oceans. Therefore, although Sm–Nd and Lu–Hf systems have evolved coherently in the continents and mantle, showing positive covariations that reflect the fractionation of Sm/Nd and Lu/Hf ratios during mantle melting and continent generation (Figure 1), manganese nodules fall off this "crust–mantle correlation" to high hafnium-isotope ratios for a given neodymium-isotope ratio. White *et al.* (1986) suggested that a significant portion of marine hafnium is derived from the mantle through hydrothermal activity, or subaerial or subaqueous weathering of volcanics. Furthermore, they suggested a low continental flux of hafnium due to retention in zircon. Despite the interest generated by surprisingly high hafnium-isotope ratios, the next study was not published for 11 yr (Godfrey *et al.*, 1997). This delay was mainly due to the difficulties of analyzing hafnium-isotope ratios by thermal-ionization mass spectrometry, a consequence of the high first-ionization potential for hafnium. This situation changed in the mid-1990s with the development of multiple collector inductively coupled plasma-source mass spectrometers.

All of the early investigators, with the exception of Harry Elderfield, were mainly mantle or planetary geochemists, and these isotopic studies had relatively small impact on the oceanography community. Nevertheless, the stage was set for future studies. The gross characteristics of the marine lead-isotopic variability was outlined by the mid-1970s based on Fe–Mn sediments as seawater proxies. The gross characteristics of the global geographic neodymium-isotopic variability in the oceans (Albare(c)de and Goldstein, 1992), and shown in Figure 3, was outlined by the early 1980s.

6.17.4 NEODYMUIM ISOTOPES IN THE OCEANS

6.17.4.1 REEs in Seawater

Neodymium is a valuable tracer for oceanographic studies, as a product of radioactive decay and as an REE. They behave as a coherent group of elements whose chemical behavior is defined by filling of the 4*f* electron shell. Conventionally, REE abundances are shown in the sequence of increasing atomic number. In studies of igneous rocks, measured REE abundances are normalized to average chondritic-meteorite values, and in marine studies they are usually normalized to "average shale" (cf. Taylor and McLennan, 1985). As mentioned above, they exist in the Earth in the +3 oxidation state and display similar chemical behavior. Their relatively small chemical behavioral differences are mainly due to the effects of decreased ionic radius with higher atomic number. Two exceptions are europium and cerium. In high-oxidation environments like the oceans, cerium can exist as Ce^{+4}, in which case it forms an insoluble oxide. In low-oxidation environments such as within the Earth, europium can exist as Eu^{+2}. This rarely occurs at the Earth's surface, but it has important effects in magma chambers where Eu^{+2} is preferentially incorporated into feldspars. Magmatic fractionation of feldspar leads to a marked negative europium anomaly in convergent-margin volcanic rocks, and is a distinctive characteristic of the composition of the average upper-continental crust (e.g. Taylor and McLennan, 1985; Wedepohl, 1995; Rudnick and Fountain, 1995; Gao *et al.*, 1998). Dissolved REEs in seawater are stabilized as carbonate complexes (Cantrell and Byrne, 1987). The fraction of each REE that exists as a carbonate complex increases with increasing atomic number.

As a result of these factors, the REE pattern of seawater is distinctive. The seawater pattern is heavy REE enriched (e.g., Elderfield and Greaves, 1982). In addition, cerium shows a marked depletion compared with its neighbors, lanthanum and praseodymium. Because average shale contains a negative europium anomaly compared to chondrites, the practice of normalizing seawater to

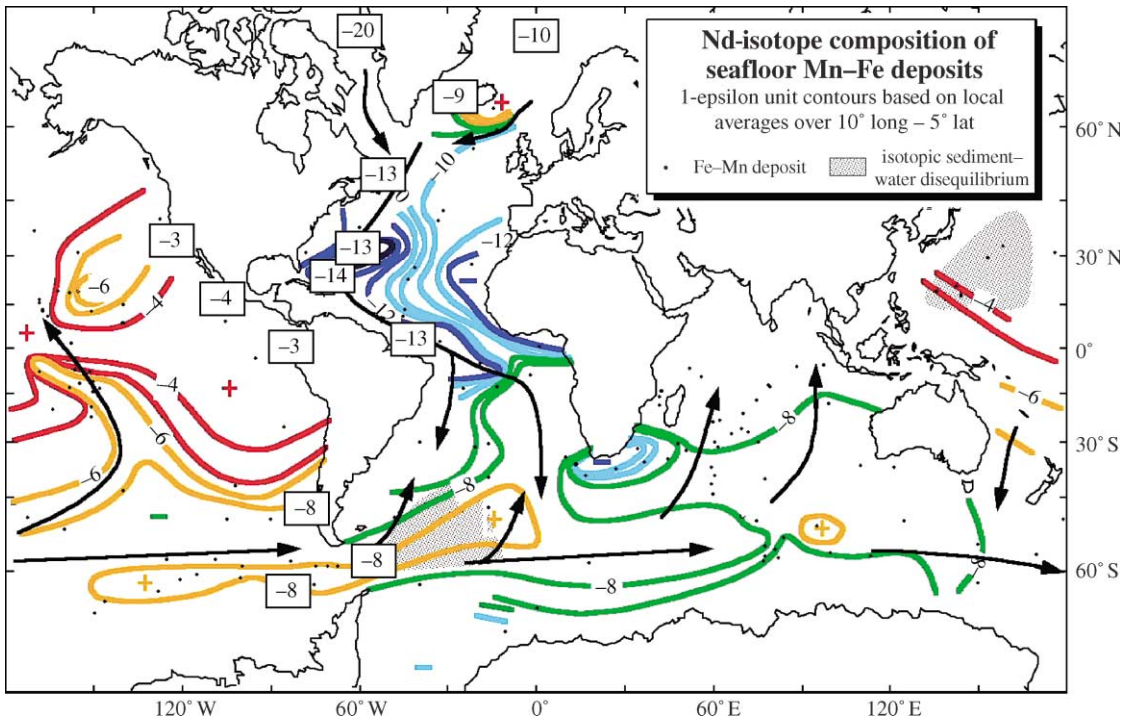

Figure 3 *Map of Nd-isotope variability in ferromanganese deposits.* The map shows systematic geographic variability with lowest values in the North Atlantic, highest values in the Pacific, and intermediate values elsewhere. Arrows illustrate general movement of deep water, and show that the contours generally follow deep-water flow. Shaded fields delineate regions where the Fe–Mn and deep seawater data differ by $>2\varepsilon_{Nd}$ units (after Albare(c)de and Goldstein, 1992).

shale mutes the magnitude of the europium anomaly in patterns normalized to shale, such as published seawater REE diagrams, as compared to patterns normalized to chondrites. Nevertheless, variability in the magnitude of europium anomalies in different source rocks causes Eu/REE ratios in seawater to vary more than the trivalent REEs. The most recent general review of REEs in the oceans is by Elderfield (1988).

Abundances of REE's in depth profiles, with the exception of cerium, generally show depletions in surface waters and enrichments in deep water. Moreover, concentrations are generally lower in the North Atlantic and higher in the Pacific. With respect to both of these characteristics they are similar to SiO_2, and REE abundances of intermediate and deep waters tend to correlate with silicate (Elderfield and Greaves, 1982; Debaar *et al.*, 1983, 1985). Nevertheless, despite similarities in the behavior of SiO_2 and the REE, there are important differences, with the Atlantic generally having higher REE/SiO_2 than the Pacific (cf. Elderfield, 1988, and references therein). Despite these inter-ocean differences, silicate is often used as a proxy for REE behavior in the oceans. As shown below, neodymium-isotope ratios place important constraints on the mode of REE cycling in the oceans.

6.17.4.2 Neodymium-isotope Ratios in Seawater

There are only a small number of published papers, fewer than 20, reporting neodymium-isotope ratios in seawater. The early work was entirely carried out in the lab of Professor Gerald Wasserburg at Caltech (Piepgras and Wasserburg, 1980, 1982, 1983, 1985, 1987; Stordal and Wasserburg, 1986; Spivack and Wasserburg, 1988), which deserves credit for mapping the primary variability in seawater. All of the other published data are from Cambridge, Harvard, Lamont, Tokyo, and Toulouse. A map of the locations of seawater data is shown in Figure 4. The reason for the small number of studies is that the task is analytically challenging, due to the very low abundance of neodymium in seawater, which generally ranges ~15–45 pmol kg^{-1} (~2–7 ng L^{-1}). Most isotope laboratories measure neodymium as a positive metal ion (Nd^+), and are comfortable measuring 80–100 ng of neodymium, which would require processing of 10–40 L of seawater per sample. For this reason most of the seawater neodymium-isotope ratios in the literature were measured as a positive metal oxide (NdO^+), which affords higher efficiency of ion transmission and allows measurements of smaller samples. Even so,

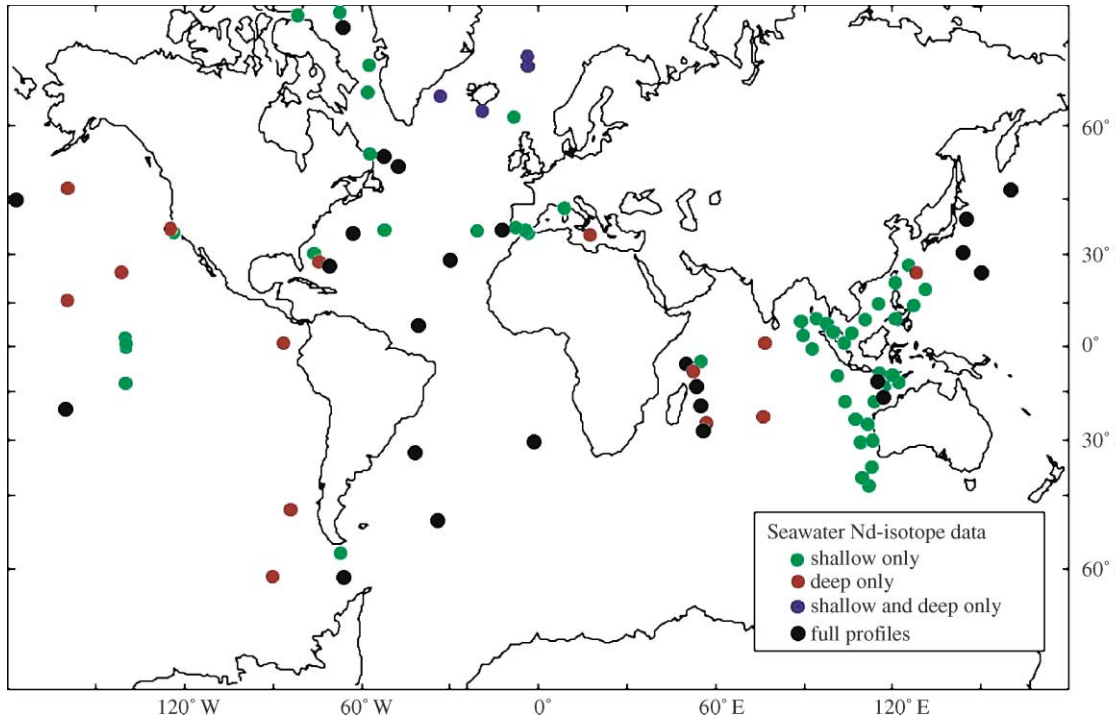

Figure 4 *Map of locations of published seawater Nd-isotope data.* Locations are distinguished by shallow-only data, deep-only data, deep- and shallow-only data, and full profiles, where "shallow" is <2,000 mb sl. All publications are cited in the text except Henry *et al.* (1994), which reports the two central Mediterranean sites.

measurements of ~15–20 ng of neodymium still require processing of 3–10 L of seawater per sample.

The variability of neodymium isotopes in the oceans is closely related to global ocean circulation. The present-day mode of thermohaline circulation has been likened to a "great ocean conveyor" (Broecker and Peng, 1982; Broecker and Denton, 1989) in which deep water formed in the North Atlantic flows southward where it enters the circum-Antarctic. Circumpolar water flows to the Indian and Pacific, where it upwells. The North Atlantic is recharged by the surface-return flow from the Pacific through the Indonesian Straits and the Indian Ocean, and by northward movement of intermediate and deep water in the Atlantic from the circum-Antarctic (Rintoul, 1991). In the latter case, southward flowing NADW (North Atlantic Deep Water) is "sandwiched" by northward flowing Antarctic bottom water (AABW) and Antarctic Intermediate Water (AAIW). The principal observations on the variability of neodymium-isotope ratios globally are summarized below, with the publications that made the main discoveries.

Neodymium-isotope ratios in deep seawater show the same general geographical pattern as in Fe–Mn nodules and crusts. The global geographical pattern is illustrated in the Fe–Mn nodule-crust map (Figure 3), and by some depth profiles (Figure 5). The North Atlantic is characterized by low values, the Pacific by high values, and the Indian Ocean is intermediate (Piepgras and Wasserburg, 1980, 1987; Bertram and Elderfield, 1993). In addition, neodymium-isotope ratios in the circum-Antarctic are also intermediate to the North Atlantic and Pacific (Piepgras and Wasserburg, 1982). Typical values are in the range of Fe–Mn nodules and crusts as noted above. The same studies show that neodymium concentrations are generally highest in the Pacific and lowest in the Atlantic (Figure 6).

NADW has a narrow range of $\varepsilon_{Nd} = -13$ to -14 (Figure 5), which defines most of the mid-range and deep water in the North Atlantic south of ~55° N (Piepgras and Wasserburg, 1980, 1987). The uniformity is perhaps surprising considering the variability of NADW sources. NADW is a mixture of sources displaying two very different neodymium-isotope components. Baffin Bay between the Labrador and Greenland receives its neodymium from old continental crust with very low neodymium-isotope ratios of $\varepsilon_{Nd} < -20$. NADW sources from the Norwegian and Greenland Sea sources east of Greenland have much higher neodymium-isotope ratios of $\varepsilon_{Nd} = -7$ to -10, and these higher values are observed in the Denmark Straits and Faeroe Channel overflow (Stordal and Wasserburg, 1986).

Surface waters show more variable neodymium-isotope ratios than intermediate and deep waters (Figure 5). In contrast to the dominance

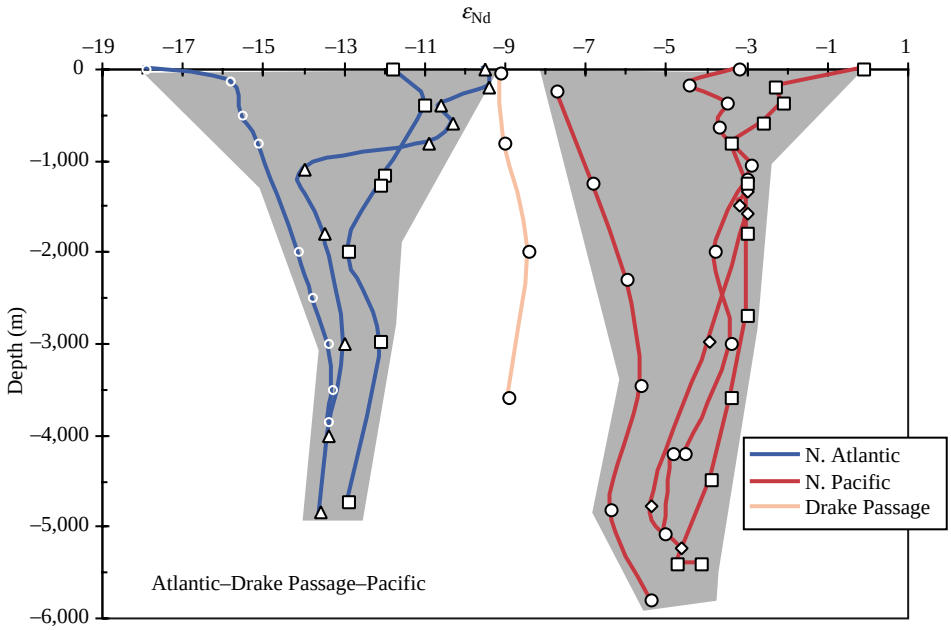

Figure 5 *Representative depth profiles of Nd-isotope ratios from the North Atlantic and Pacific oceans and the Drake Passage.* The Atlantic and Pacific profiles were chosen to encompass the range of values for deep water in those oceans. Symbols show the data. The diagram illustrates the differences between the oceans and the greater variability of Nd isotopes in shallow versus deep waters (sources Piepgras and Wasserburg, 1982, 1983, 1987; Spivack and Wasserburg, 1988; Piepgras and Jacobsen, 1988; Shimizu *et al.*, 1994).

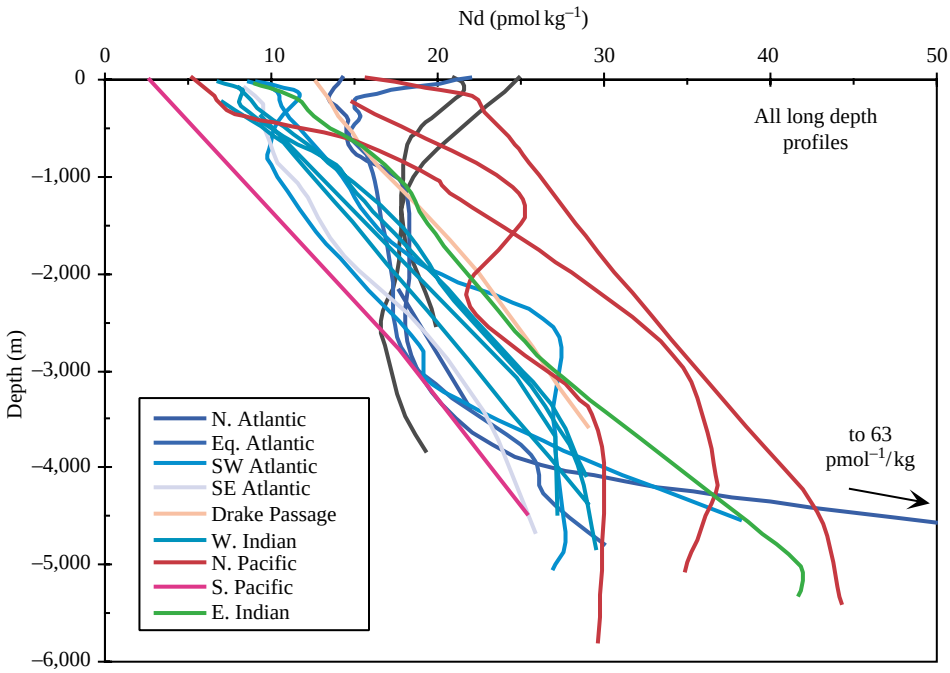

Figure 6 *Nd concentrations versus depth for all long depth profiles in the literature.* The data show that higher concentrations with depth are a general feature in the oceans, although this is not necessarily the case in the North Atlantic. Deep waters generally have the highest abundances of Nd in the North Pacific, and the lowest in the North Atlantic, but there are several exceptions (sources Piepgras and Wasserburg, 1980, 1982, 1983, 1987; Spivack and Wasserburg, 1988; Piepgras and Jacobsen, 1988; Bertram and Elderfield, 1993; Jeandel, 1993; Shimizu *et al.*, 1994; Jeandel *et al.*, 1998).

of NADW values ($\varepsilon_{Nd} = -13$ to -14) in the intermediate and deep water of the North Atlantic, surface waters are variable, ranging from $\varepsilon_{Nd} = -8$ to -26 (Piepgras and Wasserburg, 1980, 1983, 1987; Spivack and Wasserburg, 1988; Stordal and Wasserburg, 1986). The greater variability of surface waters is observed throughout the oceans. Like silicate, neodymium abundances are generally depleted in surface waters compared to intermediate and deep water (Figure 6).

The limited seawater data from the circum-Antarctic display uniform neodymium-isotope ratios intermediate to the Atlantic and Pacific ($\varepsilon_{Nd} = -8$ to -9). The only neodymium-isotope data available are from two profiles in the Drake Passage and one in the eastern Pacific sector (Piepgras and Wasserburg, 1982).

Where depth profiles sample different water masses, neodymium-isotope ratios vary with the water mass. In South Atlantic intermediate and deep water, neodymium-isotope ratios are generally intermediate to the NADW and Drake Passage values. Depth profiles show a zig-zag pattern (Figure 7), higher at intermediate depths dominated by AAIW, lower at greater depths dominated by NADW, and higher at deepest levels dominated by AABW (Piepgras and Wasserburg, 1987; Jeandel, 1993). A published diagram from von Blanckenburg (1999) overlaying neodymium-isotopic profiles and salinity (Figure 8) elegantly shows that the general characteristics of neodymium-isotope ratios vary with salinity in southward and northward flowing-water masses in the Atlantic.

Pacific intermediate and deep water dominantly display high values, of $\varepsilon_{Nd} = -2$ to -4 (Piepgras and Wasserburg, 1982; Piepgras and Jacobsen, 1988; Shimizu *et al*., 1994). Near southern Chile, and in the west-central Pacific, where circumpolar deep water moves northward, neodymium-isotope ratios display lower values closer to those typical of circumpolar seawater. In the central Pacific the circumpolar neodymium-isotope signal can be detected as far north as ~40° N (Shimizu *et al*., 1994).

Neodymium-isotope ratios of intermediate and deep water in the Indian Ocean are intermediate to the Atlantic and Pacific. They generally fall between $\varepsilon_{Nd} = -7$ to -9, and are consistent with domination by northward flowing circumpolar water (Bertram and Elderfield, 1993; Jeandel *et al*., 1998). A depth profile east of southern Africa (Figure 7) displays the same zig-zag pattern as South Atlantic intermediate and deep water, reflecting advection of NADW into the western Indian Ocean (Bertram and Elderfield, 1993).

The broadest characteristics can be concisely summarized. Neodymium-isotope ratios in seawater vary systematically with location throughout the oceans, high in the Pacific, low in the Atlantic, and intermediate in the Indian and circum-antarctic. In addition, they are variable in depth profiles that contain different water masses, and neodymium-isotope ratios associated with end-members of water masses are conserved over long advective pathways.

6.17.4.3 Where does Seawater Neodymium Come From?

The first-order question arising from the global variability is, where does the neodymium in seawater come from? The negative ε_{Nd} values clearly show that throughout the oceans the dissolved neodymium is dominantly derived from the continents (cf. Figure 1). The characteristic values in the Atlantic and Pacific indicate at first glance that they reflect the age of the surrounding continental crust. The North Atlantic, surrounded by old continental crust, has the lowest values, and the Pacific, surrounded by orogenic belts has the highest values. However, the relationships are not simple ones.

In the North Atlantic, the present-day neodymium-isotope ratio of NADW of $\varepsilon_{Nd} \approx -13.5$ is determined by efficient mixing of two disparate sources to the west and east of Greenland. The Baffin Bay source with $\varepsilon_{Nd} < -20$ is easily explained by the surrounding early and middle Precambrian continental crust. The high ε_{Nd} value of -7 to -9 of the Denmark Straits–Norwegian Sea sources are less easy to explain. Both Greenland and Norway are primarily surrounded by Precambrian continental crust, whose early to mid-Proterozoic average age suggests an average ε_{Nd} much more negative. The only substantial sources of higher neodymium-isotope ratios in the region are Iceland and the flood basalts of the British Tertiary Province, although these cover a minor portion of the surrounding land area. Unless there is a significant input into the Denmark Straits–Norwegian Sea derived from the Pacific and leakage into these regions through the Arctic, the high neodymium-isotope ratios almost certainly show substantial input from these local volcanic sources. As mentioned previously, the value of $\varepsilon_{Nd} \approx -13.5$ that characterizes NADW is the signature imparted to most of the intermediate and deep water throughout the North Atlantic south of ~55° N. The observation that the Baffin Bay–Denmark Straits–Norwegian Sea sources are so different implies that this distinctive present-day NADW signature is inherently unstable and may easily be subject to change with time.

In the Pacific, the mechanism through which seawater obtains its high neodymium-isotope ratios is not well identified. The source is clearly not from the surrounding continental masses. The major Pacific sediment sources from the surrounding

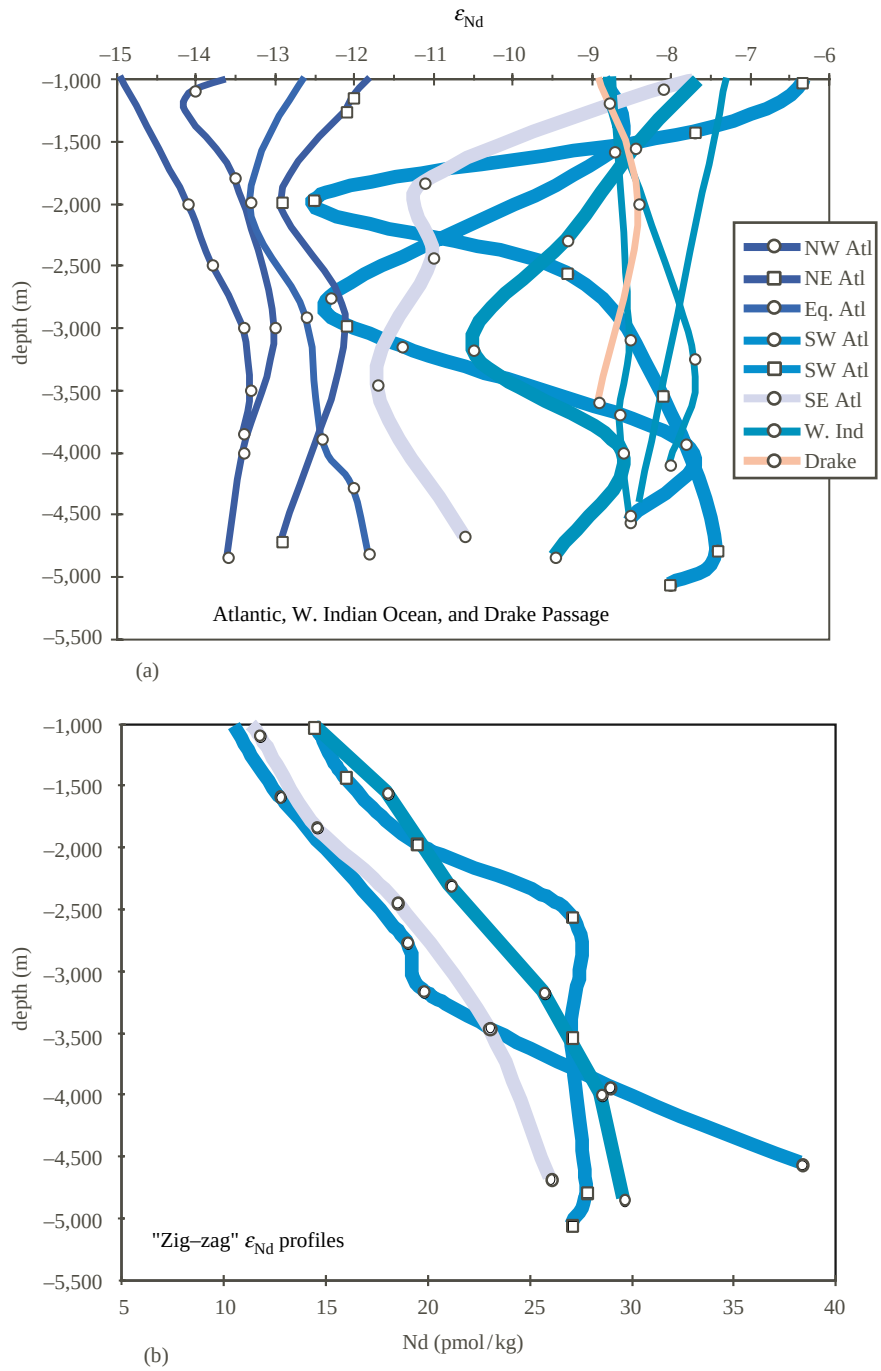

Figure 7 *Nd-isotope ratios and concentrations versus depth in the Atlantic and western Indian Oceans, and the Drake Passage.* (a) Only full profiles are shown. Western Indian Ocean data are similar to the single profile from the Drake Passage, but at slightly higher Nd-isotope ratios, which may indicate that the Drake Passage profile does not give the upper limit for the circum-Antarctic. Profiles from the South Atlantic and one from the West Indian show large variations with depth, which can range from near North Atlantic values, reflecting NADW, to near circumpolar-West Indian values, reflecting AABW and AAIW in individual profiles. (b) Nd concentrations of those profiles showing zig-zag ε_{Nd} patterns. The zig-zag profiles show that the Nd-isotopic signature of water masses is conserved over the transport path in the Atlantic (sources Piepgras and Wasserburg, 1982; 1987; Spivack and Wasserburg, 1988; Bertram and Elderfield, 1993; Jeandel, 1993).

continental crust, including all of the major rivers as well as wind-blown dust from China that is the main detritus source for the central Pacific, have much lower neodymium-isotope ratios than the typical Pacific seawater value of −4 (e.g. Goldstein *et al.*, 1984; Goldstein and Jacobsen, 1988; Nakai *et al.*, 1993; Jones *et al.*, 1994). Among Pacific land masses, the only major

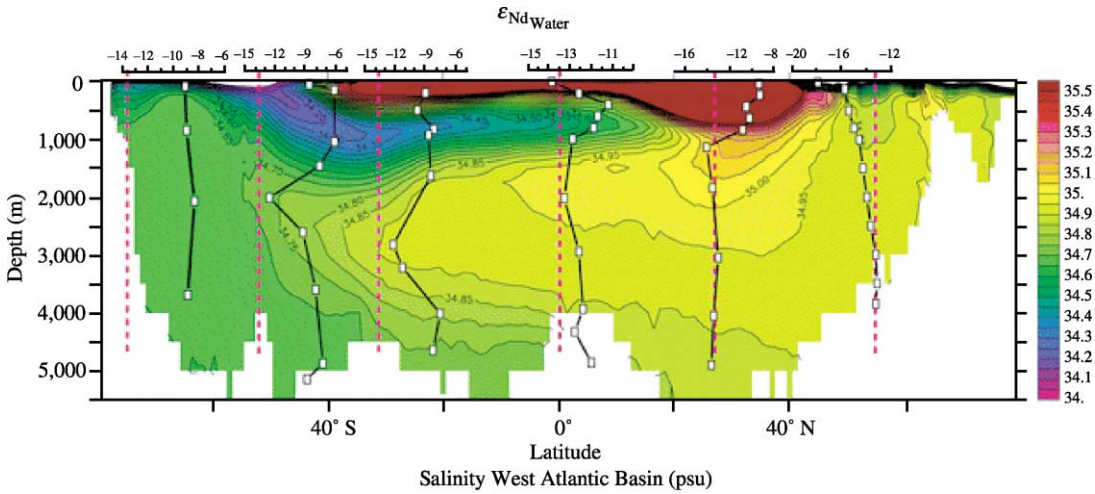

Figure 8 *Nd-isotope ratio and salinity profiles in the Atlantic*. Nd-isotope ratios with depth are consistent with salinity in the Atlantic, further showing that the Nd-isotopic signatures of water masses are conserved with advective transport (source von Blanckenburg, 1999).

sediment source with comparable neodymium-isotope ratios is Taiwan, and this has been suggested as the source of the high neodymium-isotope ratios of Pacific seawater, owing to its anomalously high erosion rate (Goldstein and Jacobsen, 1988). However, it is noteworthy that the detrital component of western and central Pacific sediments is $\varepsilon_{Nd} \approx -10$ to -12 (Nakai *et al*., 1993) and this signature is neither imparted to coexisting seawater or Pacific Fe–Mn oxide precipitates. Indeed, if the continents surrounding the Pacific were the major source of dissolved neodymium, Nd-isotope ratios in the Pacific and Atlantic would be at most only marginally different. Early studies of the REEs (Michard *et al*., 1983) and neodymium-isotope ratios in hydrothermal solutions (Piepgras and Wasserburg, 1985) from Pacific seafloor spreading axes showed that ridge volcanism cannot be a significant source of Pacific seawater neodymium. The most likely source of high neodymium isotope ratios in the Pacific is circum-Pacific volcanism. Volcanic ash is widely dispersed in the Pacific as small highly reactive particles with large surface area, and Pacific sediments have large numbers of ash layers. The Pacific Ocean is surrounded by convergent plate margins, and especially in the northwest Pacific the volcanoes lie upwind. In addition, the Pacific contains a large abundance of intraplate volcanic islands. Neodymium-isotope ratios of arc volcanics (probably the largest source) and ocean islands typically have high values of $\varepsilon_{Nd} \approx +7$ to $+10$. The effects of exchange between volcanic par ticles and seawater have been inferred from studies of neodymium isotopes in waters passing through the Indonesian Straits (Jeandel *et al*., 1998; Amakawa *et al*., 2000), and Papua New Guinea (Lacan and Jeandel, 2001). In the cases, increases in neodymium-isotope ratios along water advection pathways are attributed to local volcanic sources. Thus, it is likely that addition of neodymium from volcanic particles imparts the distinctive neodymium-isotopic fingerprint to Pacific seawater, which is ultimately intermediate to values of recent volcanic and old continental sources.

The inefficiency of neodymium exchange between continental detritus and seawater is clearly seen in the Indian Ocean. The major sources of sediment to the Indian Ocean are the Ganges–Brahmaputra and Indus river systems, with $\varepsilon_{Nd} \approx -10$ to -12 (Goldstein *et al*., 1984), whose neodymium-isotope ratios are reflected in the Bengal Fan (e.g. Bouquillon *et al*., 1990; Galy *et al*., 1996; Pierson-Wickmann *et al*., 2001). The neodymium-isotope ratio of Indian seawater is $\varepsilon_{Nd} \approx -8$, significantly higher than these sediment sources, even in Indian water close to the Indus and Bengal fans. This difference exists despite the high abundance of neodymium in continental sediment (~30 ppm) compared to Indian seawater (~0.003 ng g^{-1}), which shows that a small amount of exchange in regions with high sedimentation rates like these two Fans should have a major local effect on seawater neodymium. The fact that the large difference persists between the fan sediments and proximal Indian seawater shows that the neodymium in terrigenous detritus is tightly bound to the sediment. The neodymium-isotope ratios of Indian seawater are the same as the circum-Antarctic, as observed in direct seawater measurements and in Fe–Mn oxides. This is consistent with Indian Ocean hydrography, which shows that Indian intermediate and deep seawater is primarily fed by northward advecting water from the circum-Antarctic.

These observations, taken together, indicate that the neodymium-isotope ratios of intermediate and deep seawater are imprinted mainly in the Atlantic and Pacific oceans. The circum-Antarctic is fed by both and its intermediate neodymium-isotope ratio reflects those of the Atlantic and Pacific water sources. Indian Ocean intermediate and deep water is fed primarily by the circum-Antarctic and tends to retain a circum-Antarctic neodymium-isotope ratio.

6.17.4.4 Neodymium Isotopes as Water-mass Tracers

How well do neodymium-isotope ratios trace water masses? The apparent answer is that neodymium isotopes trace them very well. Where there is a significant neodymium-isotopic contrast between water masses with depth at a single location, as in the South Atlantic, neodymium-isotope ratios vary coherently with the water mass (Figures 7 and 8). The North Atlantic profiles show uniform ε_{Nd} values between −12 and −14 at depths >2,500 m. The Drake Passage profile shows a uniform ε_{Nd} value of ~−9. In this context, Equatorial Atlantic neodymium-isotope ratios are slightly higher than those in the North Atlantic, especially in deep water, consistent with addition of some AABW. In the South Atlantic, profiles show a strong zig-zag pattern. The lowest values nearly reach those of NADW, strongly indicating that NADW keeps its neodymium signature as it travels southward in the Atlantic. In the SE Atlantic, the NADW wedge can be identified in Figures 7 and 8, shallower than in the SW Atlantic. At shallower depths than the NADW "wedge," neodymium-isotope ratios increase toward circumpolar values in northward flowing AAIW. At deeper depths than the NADW "wedge," the neodymium-isotope ratios increase toward circumpolar values in northward flowing AABW.

The highest neodymium-isotope ratios in the South Atlantic at depths greater than 2,500 m reach ε_{Nd} ~−7.5, which are higher than the Drake Passage values (Figure 7). This may indicate a source of neodymium with high isotope ratios in the South Atlantic. However, it is premature to conclude that deep South Atlantic neodymium-isotope ratios "overstep" the Southern Ocean values, for the following reasons. The maxima for all of the deep South Atlantic waters are between $\varepsilon_{Nd} = -7$ to −9, more variable than presently available data from the Drake Passage but still quite similar. This range is also similar to circumpolar Fe–Mn sediments (Albare(c)de *et al.*, 1997). Depth profiles from the western Indian Ocean near southern Africa are similar to the South Atlantic and Drake Passage, but like the South Atlantic they slightly exceed the Drake Passage values (Figure 7). Of the three long profiles in the literature (Bertram and Elderfield, 1993), two are relatively constant ε_{Nd} with depth, while the third shows a similar zig-zag as the South Atlantic, and reflects the flow of NADW around southern Africa. It is noteworthy that the Drake Passage profile (from Piepgras and Wasserburg, 1982), is the only one in the literature from the true circum-Antarctic, and its deepest sample is from a relatively shallow depth of ~3,500 m. Either Drake passage seawater has more variable Nd isotope ratios than indicated by presently available data, or there is some addition of Nd to the circumpolar Atlantic sector from a high ε_{Nd} source.

In the global ocean, neodymium-isotope ratios in deep water (here considered to be >2,500 m) show remarkably good covariations with salinity and silicate (Figure 9), which provides key evidence of its value as a water-mass tracer. In the Atlantic and western Indian oceans, deep seawater faithfully records mixing between northern- and southern-derived water masses (Figure 10(a)). With northern waters characterized by low ε_{Nd} and high salinity, and southern waters by high ε_{Nd} and low salinity, the data show a very good covariation between the end-members and fall within a mixing envelope. Of particular interest are the data from the southwest Atlantic, where the high salinity waters fall well within the range of the north Atlantic data, and the low salinity waters within the range of South Atlantic–Drake Passage–West Indian Ocean data. A similar relationship also holds between SiO_2 and ε_{Nd} (Figure 10(b)), where northern source deep waters have low SiO_2 and ε_{Nd}, and southern source waters high SiO_2 and ε_{Nd}. Here again, most of the Atlantic data fall within a mixing envelope between the two end-members.

The Pacific is more of a homogenous pool of water than the Atlantic, and relationships between neodymium-isotope ratios and water masses are not as clearcut. Nevertheless, there is strong evidence that neodymium isotopes behave here too as conservative water-mass tracers. To the east of New Zealand there is a tongue of deep circumpolar water that moves northward. In depth profiles from the south central Pacific, the neodymium-isotope ratios of deep water reaches circumpolar values, while the intermediate water is more Pacific-like. More compelling evidence for the mainly conservative nature of neodymium in deep water is illustrated by comparing neodymium isotopes and silicate in Pacific and circumpolar waters (Figure 11). They show a good positive correlation, consistent with mixing between Pacific and circumpolar waters. In the Pacific region salinity cannot be used as a water-mass

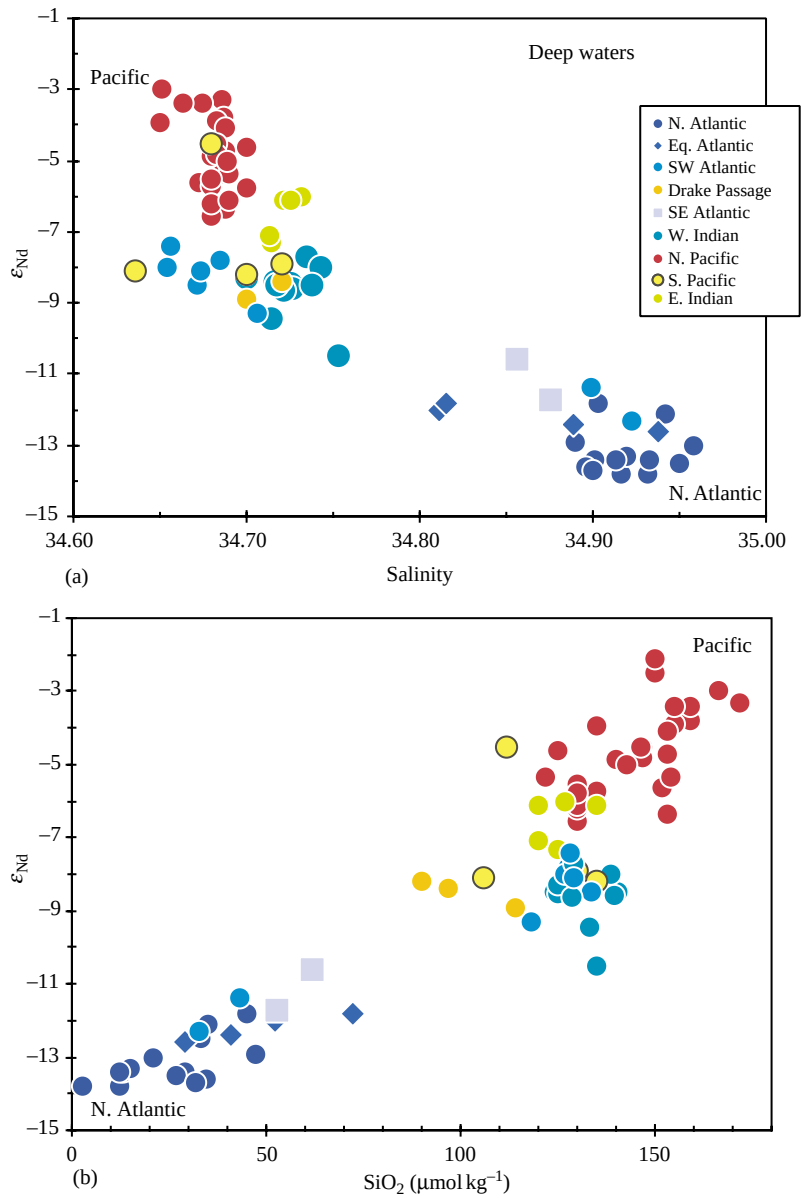

Figure 9 *Nd-isotope ratios versus salinity and silicate in deep seawater.* (a) Seawater Nd-isotope ratios display a good covariation with salinity, but the correlation breaks down somewhat in the Pacific, because its salinity is similar to the circum-Antarctic and South Atlantic. (b) Throughout the oceans there is a very good covariation with SiO_2. In both diagrams, the South Atlantic data responsible for the zig-zag patterns in profile (Figure 8) are also consistent with salinity and silicate, with high and low ε_{Nd} reflecting AABW and NADW, respectively. Thus, the Nd-isotope ratios trace the water masses of the present-day deep oceans very well. Plotted data are from >2,500 mb sl, except two Drake Passage data from 1,900 m and 2,000 m (Nd data sources: Piepgras and Wasserburg, 1980, 1982, 1983, 1987; Spivack and Wasserburg, 1988; Piepgras and Jacobsen, 1988; Bertram and Elderfield, 1993; Jeandel, 1993; Shimizu *et al.*, 1994; Jeandel *et al.*, 1998). Where salinity or silicate were not available in the publication, they were estimated from Levitus (1994), using the location and depth of the water sample.

proxy as in the Atlantic because salinity is similar in Pacific and circum-Antarctic waters (Figure 9(a)).

Taking all of these considerations into account, the available data strongly indicate that neodymium-isotope ratios in deep water are conservative tracers of water masses. While the relationships are most clear in the Atlantic, where a large portion of the basin consists of different water masses at different depths from northern and southern sources, the relationships also hold well in the Pacific. An important further implication is

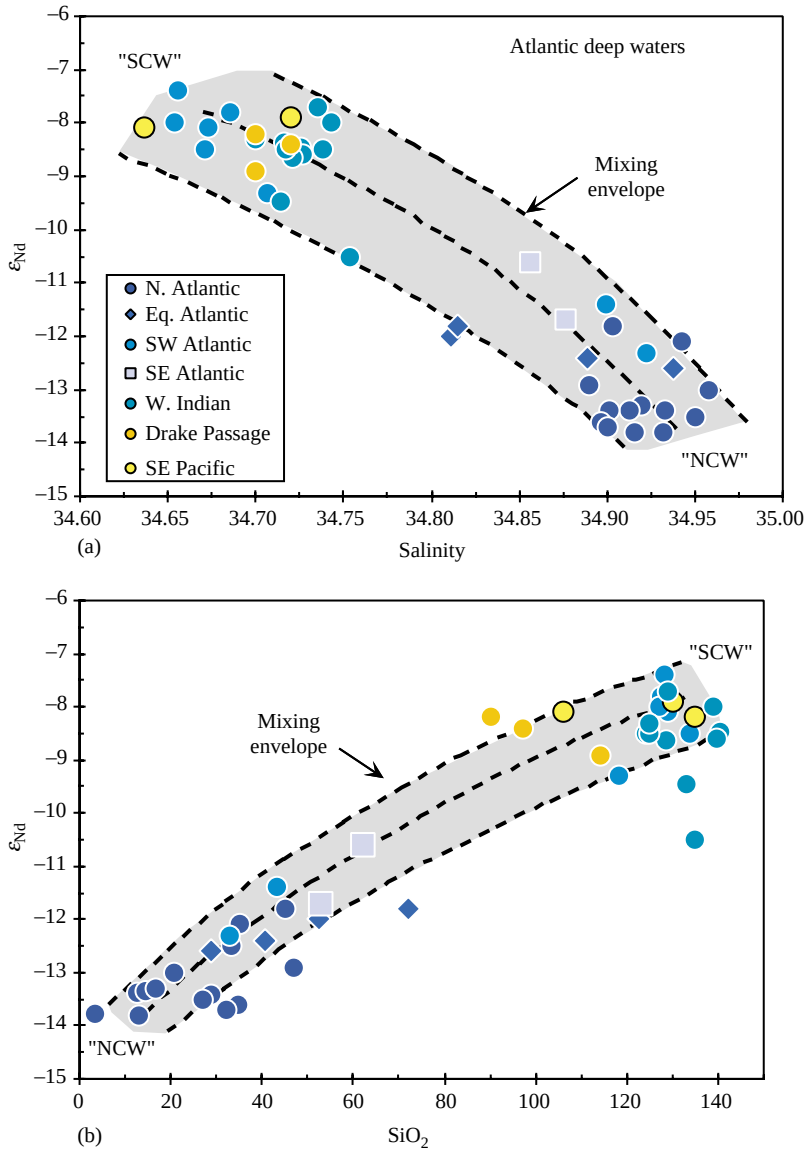

Figure 10 *Nd-isotope ratios versus salinity and silicate in Atlantic, West Indian, and Southern Ocean deep waters.* Mixing lines between northern and southern component end-member compositions (NCW and SCW, respectively) are shown, since they are nonlinear. Salinity, silicate, and Nd-isotope end-members are shown; Nd concentrations range from 16 nmol kg^{-1} to 20 nmol kg^{-1} in NCW and 27 nmol kg^{-1} to 30 nmol kg^{-1} in SCW, approximating reasonable ranges for NADW and AABW, respectively. In both (a) and (b) the data generally fall within the "mixing envelopes," showing that the Nd-isotope ratios of Atlantic deep waters reflect mixing between the northern and southern component waters. Plotted data are from >2,500 mb sl, except two Drake Passage data from 1,900 m and 2,000 m. (Nd data sources: Piepgras and Wasserburg, 1980, 1982, 1983, 1987; Spivack and Wasserburg, 1988; Piepgras and Jacobsen, 1988; Bertram and Elderfield, 1993; Jeandel, 1993). Where salinity or silicate were not available in the publication, they were estimated from Levitus (1994), using location and depth.

that neodymium isotopes should have great potential as tracers of past ocean circulation.

6.17.4.5 The "Nd Paradox"

The previous section demonstrated that neodymium-isotope ratios in the deep-ocean trace mixing between Southern and Northern Ocean waters in the Atlantic and Pacific. However, the variability of neodymium concentrations in seawater was not discussed. As noted in the discussion of REE in seawater (Section 6.17.4.1 and Figure 6), abundances generally show depletions in surface waters and enrichments in deep water, and are lower in the North Atlantic and higher in the Pacific. With respect to these characteristics the REEs are similar to SiO_2. It has already been

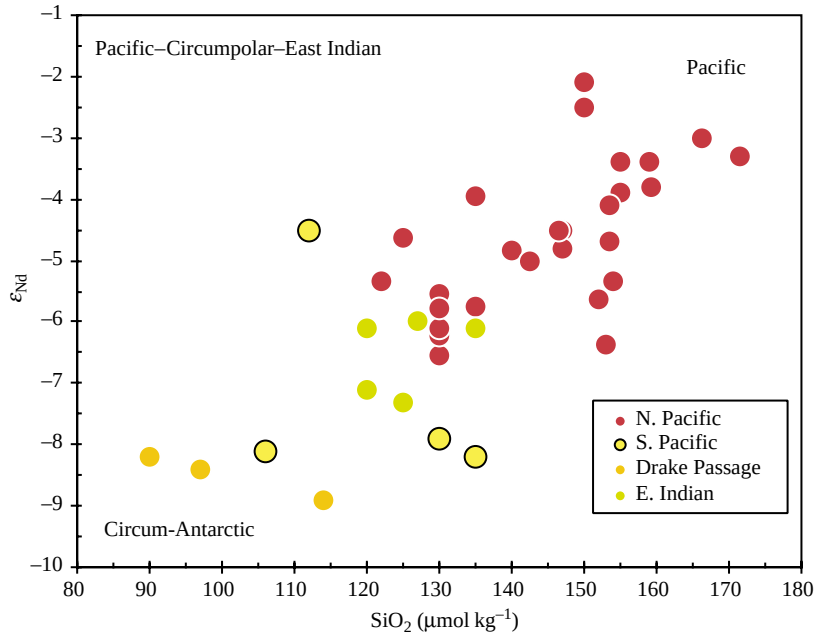

Figure 11 *Nd-isotope ratios versus silicate in Pacific, Indian, and Southern Ocean deep waters.* The positive correlation shows that Nd-isotope ratios trace mixing of deep waters from the circum-Antarctic and Pacific. Plotted data are from >2,500 mb sl, except two Drake Passage data from 1,900 m and 2,000 m (Nd data sources: Piepgras and Wasserburg, 1980, 1982; Piepgras and Jacobsen, 1988; Bertram and Elderfield, 1993; Shimizu *et al*., 1994; Jeandel *et al*., 1998). Where salinity or silicate were not available in the publication, they were estimated from Levitus (1994), using location and depth.

shown that neodymium-isotope ratios and silicate display an excellent global covariation (Figure 9(b)), and silicate is often used as a proxy for REE behavior in the oceans (e.g. Elderfield, 1988). This has been taken as evidence that silicate and Nd display a similar behavior in the oceans.

Silicate is depleted from surface waters by biological processes and remineralized in the deep water. Moreover, silicate tends to accumulate in water masses as they age (cf. Broecker and Peng, 1982). These processes account for both the increasing concentration of silicate with depth, and its increasing concentrations from the North Atlantic to the circum-Antarctic to the Pacific. With a few exceptions (notably the North Atlantic), neodymium abundances show a smooth increase with depth, and in deep water they are highest in the Pacific, lowest in the Atlantic, and intermediate in the Indian (Figure 6).

Considered separately, the neodymium-isotope ratios and the neodymium concentrations have very different implications. (i) Neodymium-isotope ratios are variable in the different oceans and within an ocean they fingerprint the advective paths of water masses. This requires that the residence time of neodymium is shorter than the ocean mixing time of $\sim 10^3$ yr (e.g., Broecker and Peng, 1982). (ii) Neodymium concentrations appear to mimic silicate, implying orders of magnitude longer residence times of $\sim 10^4$ yr and indicating increased addition through dissolution along the advected path of water masses. These observations were first addressed in detail by Bertram and Elderfield (1993), and further emphasized by Jeandel and colleagues (Jeandel *et al*., 1995, 1998; Tachikawa *et al*., 1997a,b; Lacan and Jeandel, 2001), who termed this the "Nd paradox." Both groups have suggested a general model of neodymium cycling in the oceans, that treats neodymium and the other REE as an analog to silicate. Neodymium is introduced into the surface ocean through partial dissolution of atmospheric input. For example, Jeandel *et al*. (1995) estimate that half of the global atmospheric input is dissolved when entering seawater. The cycling model suggests that in the deep-water source regions such as the North Atlantic the neodymium reaches the deep ocean through water mass subduction; elsewhere the neodymium is scavenged by organisms, vertically transported to deep water as the organisms settle in the water column, and added to the deep ocean through particulate-water exchange. Throughout the oceans neodymium is advected along with water masses. Thus, the inheritance of neodymium-isotope ratios of deep-water sources along with increasing neodymium concentrations as water ages are explained by a combination of lateral advection and vertical cycling.

It was argued above (Section 6.17.4.4) that the neodymium-isotope ratios, are conservative tracers of the advective movement and mixing of water masses (e.g., Figures 7, 10, and 11), that distinguish the southward flow of NADW and northward flow of AABW and AAIW in the Atlantic, as well as exchange between Pacific and circum-Antarctic waters. To the extent that neodymium-isotope ratios in the Atlantic and Pacific trace exchange of water between these oceans and the circum-Antarctic, they are potentially powerful oceanographic and paleoceanographic tracers. However, this implies that neodymium-isotopic signatures are imparted to deep water primarily at two locations, the North Atlantic and the Pacific, and that mixing yields intermediate neodymium-isotope ratios in the circum-Antarctic. If vertical transport from surface waters and neodymium exchange in deep waters is an important process throughout the oceans, then neodymium that is extraneous to the deep water masses must be added along the transport path. Unless the added neodymium fortuitously has the same isotope ratio as the water mass, the value of neodymium-isotope ratios as a water-mass tracer will be compromised. The extent that neodymium isotopes are compromised as water-mass tracers depends on how much the deep-water neodymium-isotopic fingerprint is changed by the addition or exchange.

A test against a significant addition of shallow neodymium to deep waters is to show that deep and shallow waters at the same location have markedly different neodymium-isotope ratios. While most published depth profiles are ambiguous in this regard, there are several published profiles in which the shallow and deep water have significantly different neodymium-isotopic signatures (Figure 12(a)). These neodymium-isotopic profiles are from all of the ocean basins; therefore, it is reasonable to infer that this relationship is a general feature of the oceans. The contrasts between deep and shallow water can be quite large, $\sim 4\varepsilon_{Nd}$ units in the Atlantic, and $\sim 8\varepsilon_{Nd}$ units in the South Pacific. Concentration profiles of the same samples show smoothly increasing neodymium abundances with increasing depth (in all cases but the North Atlantic), with deep-water concentrations generally more than a factor of 2 higher than shallow waters (Figure 12(b)). Without the constraints from the neodymium-isotope ratios, the concentration profiles are consistent with shallow scavenging of neodymium and remineralization at increasing depths. However, taken together, the differences between deep and shallow water neodymium-isotope ratios and concentrations preclude the addition of significant quantities of neodymium scavenged at shallow levels to the deep water. This means that vertical cycling at these sites does not appear to explain the higher neodymium concentrations in the deep water.

Can the Nd paradox be resolved by water-mass mixing? Vertical cycling does not appear to explain both the neodymium-isotope ratios and Nd concentrations in the oceans. Neodymium-isotope covariations with salinity and silicate in the Atlantic and Pacific are broadly consistent with mixing between northern- and southern-source waters in both basins (Figures 10 and 11). However, using the analogy to silicate, the increasing concentrations of neodymium from the Atlantic, to the circum-Antarctic/Indian, to the Pacific, have been explained in terms of increased addition of neodymium with the aging of deep water. If the high neodymium-isotope ratios of Pacific water are a result of reaction of volcanic ash with seawater, then can this could be the source of the higher neodymium concentrations in the Pacific compared to the Atlantic? Can the "Nd paradox" be explained by addition of Nd to deep water in the North Atlantic and the Pacific combined with water mass exchange between the North Atlantic–circum-Antarctic–Pacific oceans?

In terms of the global ocean, the intermediate neodymium-isotope ratios and neodymium concentrations of the circum-Antarctic/Indian oceans are not explicable through simple mixing of North Atlantic and Pacific source waters. In the circum-Antarctic and Indian oceans, neodymium concentrations are too low (Figure 13). This is reasonable, and could be a reflection of neodymium scavenging in the water column during advective transport between the North Atlantic and circum-Antarctic on the one hand, and the Pacific and circum-Antarctic on the other.

The North Atlantic and the Pacific are not directly linked, rather their linkage is modulated by the circum-Antarctic. Therefore, a more direct question is whether the neodymium-isotope ratios and concentrations are explicable in terms of binary mixing between Northern and Southern component waters within each basin. In the Pacific, it was pointed out by Piepgras and Jacobsen (1988) that neodymium-isotope ratios appear to follow simple mixing between the North Pacific and the Southern Ocean (illustrated in Figure 11) but concentrations do not. They attributed the apparent coherence of the neodymium isotopes and its absence in the neodymium concentrations to the loss of similar proportions of neodymium by scavenging from waters derived from the Pacific and circum-Antarctic during advective transport. The losses would not change the neodymium-isotope ratios, and the appearance of binary mixing systematics would be conserved.

In the Atlantic, like the Pacific, neodymium-isotope ratios are consistent with mixing of

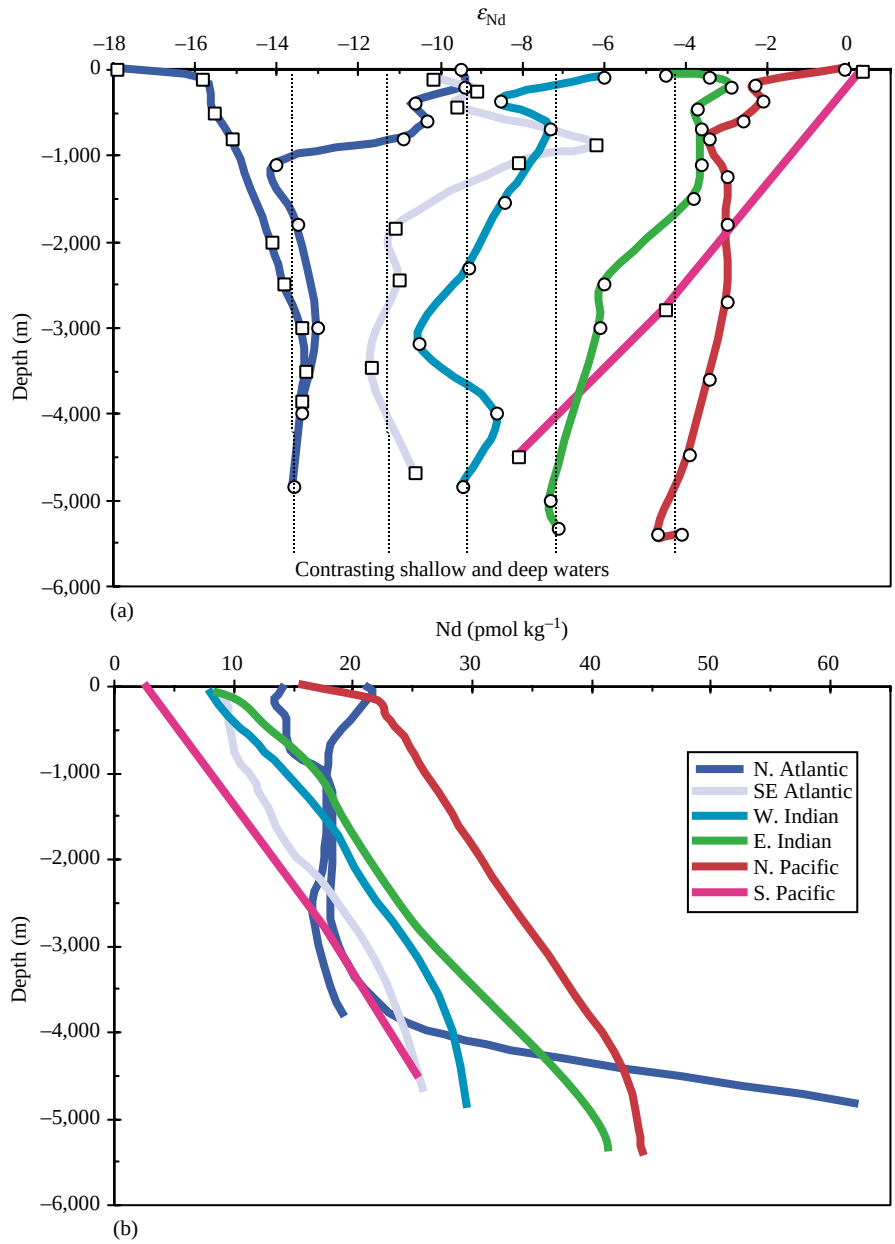

Figure 12 *Comparison of Nd-isotopes and abundances in shallow and deep waters.* (a) These examples, from all the ocean basins, highlight profiles where the Nd-isotope ratios of shallow and deep waters show large differences, as high as ~4ε_{Nd} units in the Atlantic and ~8ε_{Nd} units in the South Pacific. Dashed vertical lines emphasize the differences between the shallow and deep waters. (b) Concentration profiles show smoothly increasing Nd abundances with increasing depth in all cases but the North Atlantic. Deep-water concentrations are generally greater than twice as high as shallow waters. The abundance profiles are consistent with shallow scavenging of Nd and addition at increasing depths, but the differences between deep and shallow water Nd-isotope ratios preclude significant addition Nd scavenged at shallow levels. (Nd data sources: Piepgras and Wasserburg, 1982, 1987; Piepgras and Jacobsen, 1988; Bertram and Elderfield, 1993; Jeandel, 1993; Jeandel *et al*., 1998).

Northern and Southern end-members using salinity or silicate as conservative water-mass mixing proxies (Figure 10). Comparing neodymium-isotope ratios and concentrations, the compositions of many samples are also consistent with North–South water-mass mixing (Figure 14(a)). However, a substantial portion of the data is outside any reasonable mixing envelope. Whereas in the Pacific–circum-Antarctic case above, the non-conservative behavior of the concentrations can be explained by loss during advection, in the Atlantic the neodymium concentrations of the samples outside the mixing envelope are too high. Moreover, those that are too high tend to be

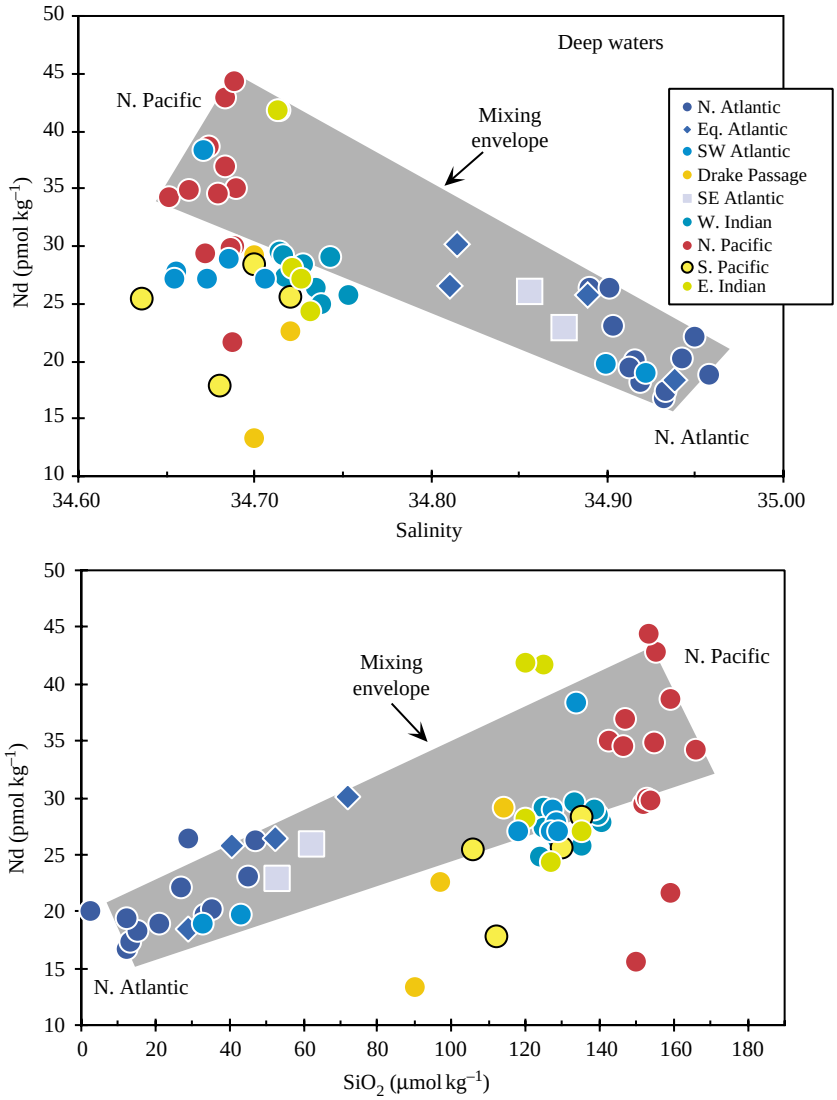

Figure 13 *Nd abundance versus (a) salinity and (b) silicate in deep seawater.* Nd concentrations do not show the same well-behaved characteristics as Nd-isotope ratios with salinity and silicate in global deep water. Mixing envelopes are shown between North Atlantic and Pacific end-members, and the circum-Antarctic, South Atlantic, and Indian Ocean samples fall outside of it. Plotted data are from >2,500 mb sl, except two Drake Passage data from 1,900 m and 2,000 m (Nd data sources: Piepgras and Wasserburg, 1980, 1982, 1983, 1987; Spivack and Wasserburg, 1988; Piepgras and Jacobsen, 1988; Bertram and Elderfield, 1993; Jeandel, 1993; Shimizu *et al.*, 1994; Jeandel *et al.*, 1998). Where salinity or silicate were not available in the publication, they were estimated from Levitus (1994), using location and depth.

the deepest samples (not shown in Figure 14 but this can be inferred from Figure 6 combined with Figure 9). The neodymium concentrations of the available data set in the Atlantic, therefore, point to an overabundance of neodymium in the deepest waters, as noted by Bertram and Elderfield (1993), and Jeandel and colleagues (Jeandel *et al.*, 1995, 1998; Tachikawa *et al.*, 1997, 1999a,b; Lacan and Jeandel, 2001). The neodymium-isotope ratios, however, place important constraints on the addition process. Figure 14(a) shows that the samples lying outside of the mixing envelope from the North Atlantic and the Equatorial Atlantic have neodymium-isotope ratios that are the same as samples within the mixing envelope. Comparison of neodymium concentrations with salinity (Figure 14(b)) shows that the same samples fall outside the simple mixing envelope. Therefore, the neodymium concentrations are enriched, but the isotope ratios are normal for the location. It was shown in Figures12(a) and (b) that depth profiles exist from all the oceans showing that high neodymium concentrations in deep water cannot be explained by addition of neodymium from

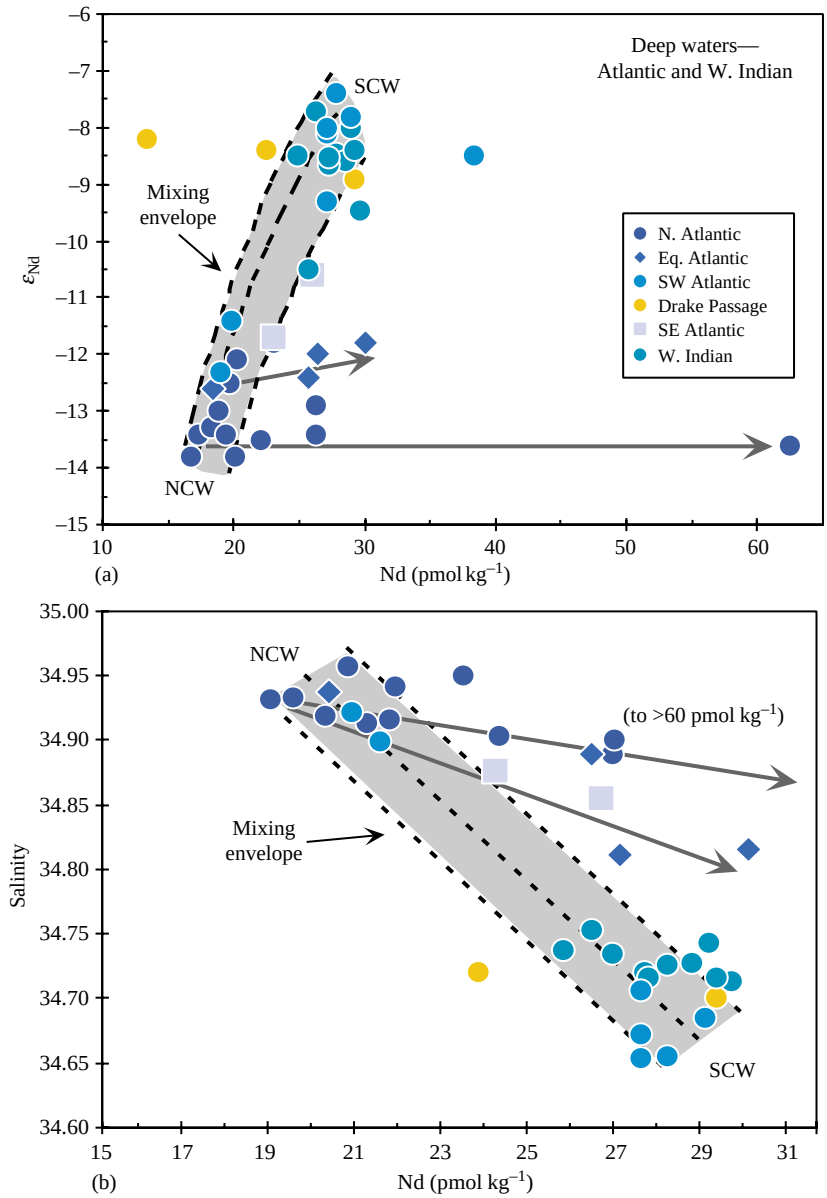

Figure 14 *Nd abundance versus salinity and silicate in deep Atlantic region seawater.* Mixing lines between northern and southern component waters (NCW and SCW) are shown in (a) because they are nonlinear. In both (a) and (b) much of the data fall within the "mixing envelopes," but many samples show high concentrations of Nd. These are generally the deepest samples. Arrows show that large increases in Nd concentrations in a region or profile are not accompanied by significant changes in Nd-isotope ratio (Nd data sources: Piepgras and Wasserburg, 1980, 1982, 1983, 1987; Spivack and Wasserburg, 1988; Bertram and Elderfield, 1993; Jeandel, 1993). Where salinity or silicate were not available in the publication, they were estimated from Levitus (1994), using location and depth.

surface waters. Profiles of ε_{Nd} and neodymium versus depth from the South Atlantic and western Indian oceans are shown in Figure 7. The concentration profiles shown in Figure 7(b) are those with zig-zag ε_{Nd} patterns. In all these cases, the neodymium concentrations increase smoothly with depth, despite the zig-zag pattern of the neodymium-isotope ratios. The neodymium-isotope ratios reflect the deep-water masses, while the neodymium concentrations appear to be decoupled.

The increasing concentrations of neodymium with depth indicate that neodymium is added to deep water as water masses laterally advect in the Atlantic, however, the neodymium that enriches deep waters along the advective path in the Atlantic has isotope ratios expected for the respective water masses. The isotope ratios appear

to preclude vertical cycling of neodymium through scavenging at shallow levels, followed by addition at deeper levels, as a primary cause of increasing neodymium concentrations with depth. The "Nd paradox" still stands.

6.17.4.6 Implications of Nd Isotopes and Concentrations in Seawater

The forgoing discussion shows that neodymium-isotope ratios are excellent conservative tracers of water masses throughout the oceans. However the processes that are controlling neodymium concentrations are still not well understood. An important avenue of further research will be to compare ε_{Nd} of authigenic and terrigenous sediments in key areas. Nevertheless, the close relationship between neodymium-isotope ratios and water masses, coupled with the range of global variability in the oceans, indicate that it can be an effective water mass tracer in the present day and shows great potential as a tracer of past ocean circulation.

6.17.5 APPLICATIONS TO PALEOCLIMATE

6.17.5.1 Radiogenic Isotopes in Authigenic Ferromanganese Oxides

The discussions (Section 6.17.4) above showed that the primary controls on the composition of neodymium-isotope ratios in seawater in crusts are the provenance (possibly modified by weathering, e.g., von Blanckenburg and Nagler, 2001) and ocean circulation. In order for a tracer to be valuable for paleoceanographic studies, its modern distribution should follow water masses in a simple way, and neodymium isotopes clearly fulfill this criterion. A world map of neodymium-isotope ratios in the outer portions of Fe–Mn nodules and crusts (Figure 3) shows that they display systematic geographical variations. In most regions they are the same as the local bottom water. A spectacular indication of the veracity of neodymium isotopes in manganese crusts and nodules as water-mass tracers is the comparison of the pattern of ^{14}C ages of bottom waters in the Pacific Ocean (Figure 15;

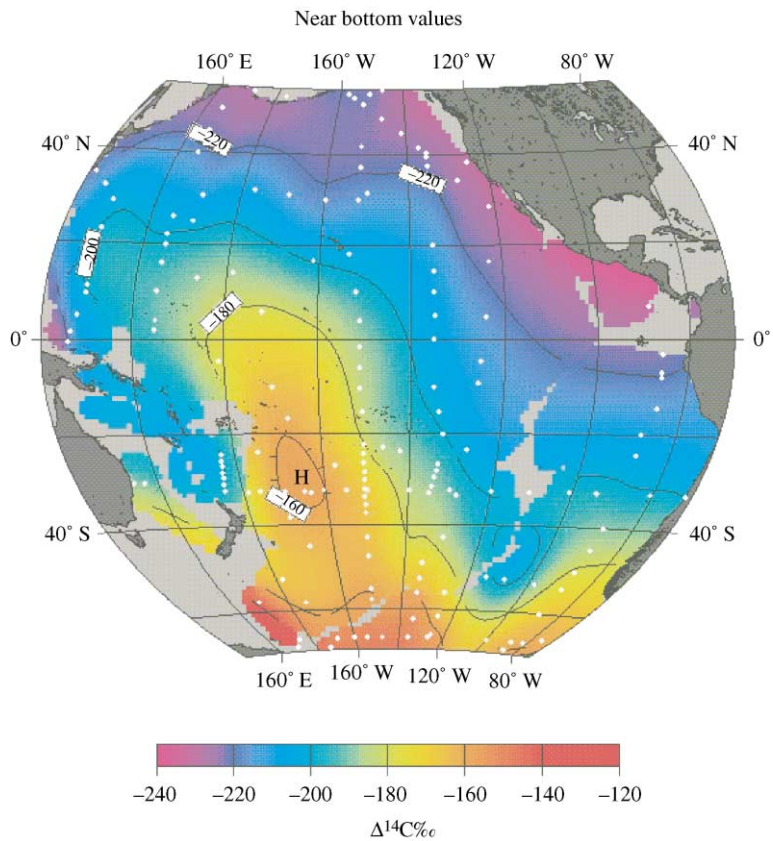

Figure 15 *$\Delta^{14}C$ in deep Pacific seawater.* The tongue of high $\Delta^{14}C$ shows the present-day path of circumpolar water entering the Pacific in the present day. The location and shape of the tongue of high ^{14}C water is similar to the "tongue" of low Nd isotope ratios in Fe–Mn deposits shown in Figure 3. In the Fe–Mn samples the low Nd isotope "tongue" is an integrated signal over 10^5–10^6 yr. The comparison shows that the Nd isotope signal in the Fe–Mn samples track the path of circumpolar water into the Pacific, and that on average the pathway has remained the same over the last million years (reproduced by permission of R. Key, Princeton University from *Ocean Circulation and Climate: Observing and Modelling the Global Ocean*, **2001**, pp. 431–452).

Schlosser *et al.*, 2001) with the world map neodymium-isotope ratios of Fe–Mn nodules and crusts (Figure 3). Manganese crusts and nodules grow at a rate of a few millimeters per million years and thus each sample generally integrates several glacial–interglacial cycles. Thus, the strong correlation with modern water-mass characteristics is a testament to the general stability of the modern ocean circulation through the Pleistocene.

However, Albare(c)de and Goldstein (1992) noted that there are some notable deviations between modern water values and crusts. Of particular note is the southwestern Atlantic region where the crust data have higher neodymium-isotope ratios than modern deep water (Figure 3). Data from disseminated authigenic neodymium from marine sediment core RC11-83, from the Cape Basin in the southeast Atlantic (Rutberg *et al.*, 2000), provides a resolution of this apparent conflict. This study traced the export of NADW to the Southern Ocean through the last glacial period to ~70 ka, and was the first to track deep-ocean circulation using neodymium-isotope ratios on glacial–interglacial timescales. It was found that the Holocene and marine-isotope stage 3 (MIS 3) record is like that predicted from the modern water column data, while the MIS 2 and 4 records are more like Pacific seawater (Figure 16). The integrated signal over the last 4 MISs is comparable to the outer portions of manganese crusts and nodules of that region. This further emphasizes that neodymium-isotope ratios in marine authigenic Fe–Mn oxides have great potential as paleoceanographic water-mass proxies.

Although lead-isotope ratios in the present-day oceans cannot be calibrated due to anthropogenic contamination, as previously discussed, one of the first major long-lived radiogenic isotope studies showed that the pre-industrial distribution can be determined using authigenic Fe–Mn sediments (Chow and Patterson, 1959, 1962). Further studies (Abouchami and Goldstein, 1995; von Blanckenburg *et al.*, 1996) have shown that lead-isotope ratios from the surface layers of Fe–Mn nodules and crusts have similar patterns to neodymium isotopes. That is, they are consistent with an older continental provenance in the Atlantic and a younger one in the Pacific, and the present-day geographical distribution is consistent with dispersion of the signals by ocean circulation.

The primary limitation of using Fe–Mn crusts for paleoceanographic studies derives from

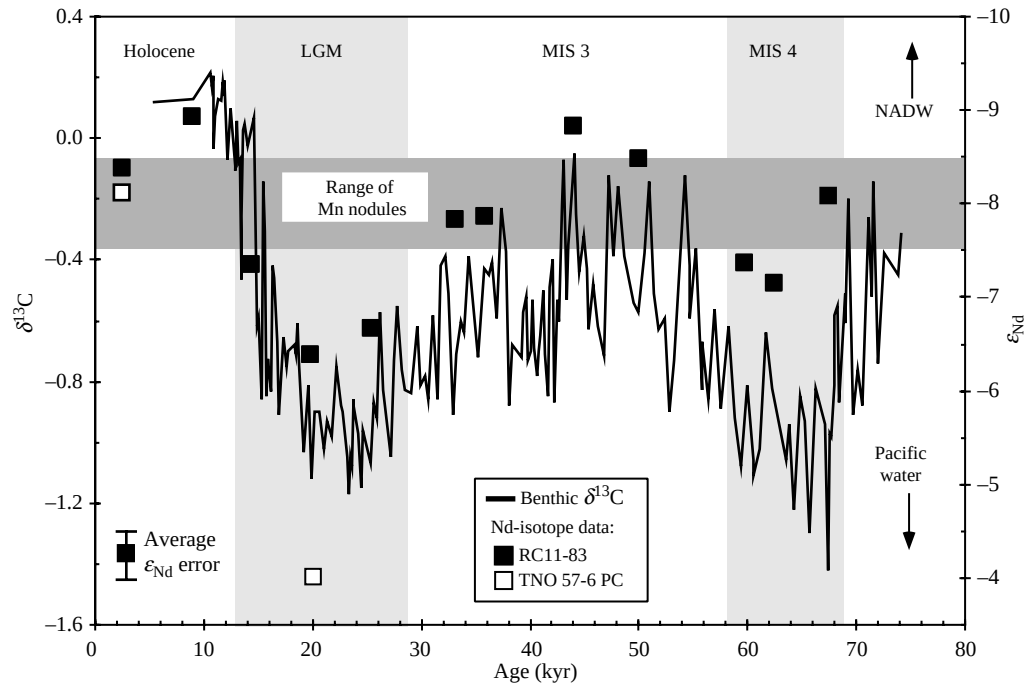

Figure 16 *Nd-isotope ratios of Fe–Mn leachates and benthic foraminiferal* $\delta^{13}C$ *versus age in southeast Atlantic cores.* The ε_{Nd} axis is reversed in order to facilitate comparison. The $\delta^{13}C$ variations were previously interpreted as reflecting changes in thermohaline circulation intensity over the Holocene and the last ice age (Charles and Fairbanks, 1992; Charles *et al.*, 1996). The down-core Nd-isotope ratios are consistent with stronger and weaker thermohaline circulation intensity during warm and cold marine isotope stages (MIS 1,3 and 2,4), respectively. In TNO57-6, located shallower and farther south than RC11-83, the glacial Nd-isotope value is like the Pacific, and may indicate a shutdown of NADW export to the circum-Antarctic. Horizontal shaded region shows the range of Nd-isotope ratios in circumpolar Fe–Mn nodules (Albare(c)de *et al.*, 1997) (after Rutberg *et al.*, 2000).

the slow growth rates, which limit the possible time resolution. The only Fe–Mn crust with an age record allowing a time resolution of a few thousand years is sample VA13-2 (cf. Segl *et al*., 1984), from the central Pacific, where significant changes on glacial and subglacial scales are not expected. A study by Abouchami *et al*. (1997) established the constancy of neodymium-isotope ratios in the Pacific through the last several glacial stages. Fe–Mn encrustations have been used extensively over the last several years to investigate long-term changes in the sources of neodymium and lead at different localities in the oceans (cf. Frank, 2002, and references therein). For higher time resolution, the record on disseminated Fe–Mn oxides in South Atlantic core RC11-83 by Rutberg *et al*. (2000) shows great future potential for addressing issues associated with changes of ocean circulation (Figure 16). In addition, Vance and Burton (1999) have concluded that they can trace changes in the provenance of neodymium in surface waters on the basis of analyses of carefully cleaned foraminifera.

6.17.5.2 Long-term Time Series in Fe–Mn Crusts

The current state of the long-term time series data from Fe–Mn crusts long-term has been addressed in detail in the review by Frank (2002). Here we only present a general summary.

On large timescales over millions of years, neodymium and lead isotopes in Fe–Mn crusts have the potential for addressing changes in weathering contributions to the ocean, major circulation changes controlled by tectonic movements of the continents, and opening or closing of important ocean passages. The isotopic signature of the input to the oceans may vary for a variety of reasons, including changes in contributions to the oceans from continental terrains of different ages, changes in runoff and elevation, and even changes in the degree of incongruent weathering. As a result, applications on long timescales are intriguing but complicated.

The review by Frank (2002) discusses the long-term time series neodymium- and lead-isotope data from 19 Mn crusts, and some clear patterns are evident. The North Atlantic and Pacific record the extreme old and young continental provenance, respectively, throughout the time span of the crusts of up to ~60 Myr, with the Indian Ocean remaining intermediate throughout. In addition, the initiation of northern hemisphere glaciation is accompanied by a dramatic trend towards older continental sources in North Atlantic crusts. The data show that the glacial erosion process yielded an increased contribution of ancient continental products to the dissolved load of the Atlantic, and possibly a higher concentration as well. Moreover, the Southern Ocean does not show a correlative change. This has been interpreted to indicate that the time-integrated (over the $\sim 10^5 - 10^6$ yr time resolution of a single Fe–Mn crust sample) contribution of NADW to the Southern Ocean decreased with the onset of northern hemisphere glaciation (Frank *et al*., 2002). Several papers have raised questions about incongruent chemical weathering imprints on the isotope composition of dissolved neodymium (von Blanckenburg and Nagler, 2001) and hafnium and lead isotopes (Piotrowski *et al*., 2000; van de Flierdt *et al*., 2002).

6.17.5.3 *Hf–Nd Isotope Trends in the Oceans*

Among long-lived isotope systems, the best correlated in continental rocks and oceanic basalts are neodymium- and hafnium-isotope ratios. They form a very coherent positive linear trend which is taken as the "mantle–crust array" (Figure 17(a)), reflecting the effects of coupled fractionation of Sm/Nd and Lu/Hf ratios through the history of the differentiation of the silicate earth (e.g. Vervoort *et al*., 1999). However, marine Hf–Nd isotopic variations lie on a slope that diverges from the crust–mantle array. While the range of ε_{Hf} values in continental rocks is about twice that of ε_{Nd}, the variability of hafnium isotopes in Fe–Mn crusts and nodules is considerably smaller than that of neodymium isotopes (White *et al*., 1986; Piotrowski *et al*., 2000; Godfrey *et al*., 1997; Albare(c)de *et al*., 1998; van de Flierdt *et al*., 2002). As a result, Nd–Hf isotope ratios of Fe–Mn crusts and nodules fall off the Nd–Hf "mantle–crust array" (Figure 17(b)), where relative to the array, the hafnium-isotope ratio is too high for a given neodymium-isotope ratio.

This observation has been interpreted in various ways. (i) The residence time of hafnium in the oceans is longer than neodymium (White *et al*., 1986). (ii) Hydrothermal systems associated with ridge volcanism make a significant contribution to the hafnium in the oceans (White *et al*., 1986), unlike neodymium (Michard *et al*., 1983; Piepgras and Wasserburg, 1985). (iii) Hafnium isotopes in seawater reflect incongruent weathering of continental rocks. This last possibility could have a large effect because hafnium is a major element in the mineral zircon, comprising a few to several percent by weight. Moreover, the high hafnium abundance in zircon means that the Lu/Hf ratio is close to zero. As a result, hafnium isotopes in zircons do not change markedly with time due to radioactive decay. Due to the high abundance,

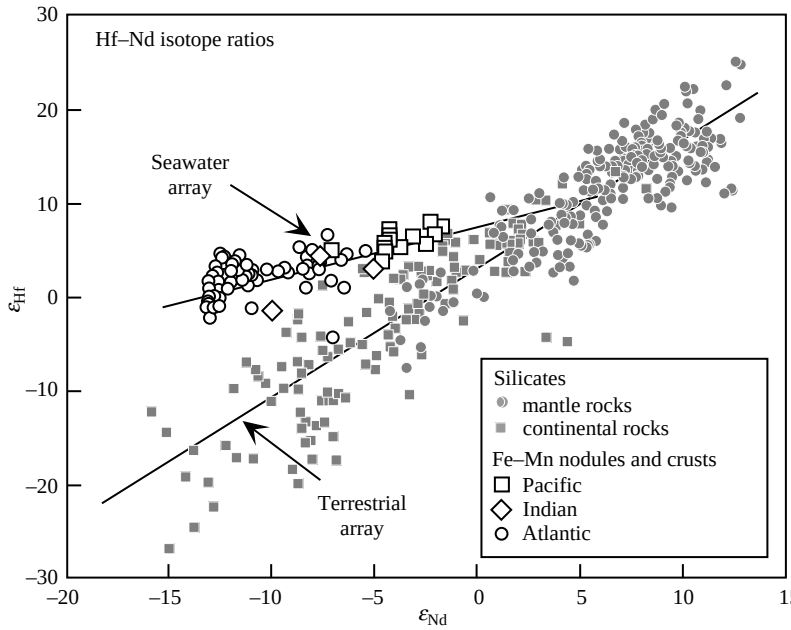

Figure 17 *Nd–Hf isotope ratios in rocks and Fe–Mn deposits.* In mantle and continental rocks these two isotope ratios a positive covariation, reflecting correlated fractionations of Sm/Nd and Lu/Hf during mantle melting and continent formation over Earth history. Seafloor Fe–Mn deposits are distinct, and lie off the continent-mantle "array," at high Hf isotope ratios for a given Nd isotope ratio. Possible explanations are given in the text. The figure is modified from van de Flierdt *et al.* (2002). The crust–mantle "array" is based on Vervoort *et al.* (1999). (Hf isotope data on Fe–Mn samples: White *et al.*, 1986; Godfrey *et al.*, 1997; Albare(c)de *et al.*, 1998; Burton *et al.*, 1999; Piotrowski *et al.*, 2000; David *et al.*, 2001; van de Flierdt *et al.*, 2002).

a significant fraction of the hafnium budget of the continental crust resides in zircon. Finally, zircon is highly resistant to weathering. As a result, hafnium may be preferentially weathered from non-zircon portion of a rock, with a significantly higher Lu/Hf and hafnium-isotope ratio (depending on the geological age) than the bulk rock (White *et al.*, 1986; Piotrowski *et al.*, 2000; Godfrey *et al.*, 1997; van de Flierdt *et al.*, 2002).

Of course, all of these factors may be partly acting to produce the marine Hf–Nd isotope trend. At first glance a longish apparent residence time for hafnium is puzzling. However, White *et al.* (1986) note that the flux of continental-derived hafnium to the oceans is likely to be quite small due to the insoluble nature of zircon and hafnium in general. They refer to a model of scavenging by particulate matter of Balistrieri *et al.* (1981) and find that if they use the relevant constants for hafnium they get scavenging residence times of the REEs of 10^2 yr, compared to 10^{12} yr for hafnium! They note that these predictions are qualitatively consistent with the observation that hafnium is only slightly enriched in deepsea red clays while rare earths are strongly enriched (Patchett *et al.*, 1984). Van de Flierdt *et al.* (2002) report a high resolution study of some North Atlantic manganese crusts, and find that at about the time of onset of northern hemisphere glaciation, the marine Hf–Nd isotope array moved steeply downward in the direction of silicate reservoirs. They further showed a systematic negative correlation between lead and hafnium isotopes. The hafnium-isotope ratios decrease and lead-isotopes increase at the time of the northern hemisphere glaciation, which is consistent with addition of both elements through greater weathering of ancient zircon. Accordingly, they provide evidence that in some cases the normally inert zircon can be ground finely enough to be partly dissolved.

Thus, it is possible that all of the three controls are acting on the hafnium contribution to seawater. Despite the low concentrations of neodymium in seawater, the high Nd/Hf ratios in Fe–Mn crusts indicate relatively lower hafnium abundances. Because zircon is not a crystallizing phase in basalts, hafnium is not sequestered in zircon in the oceanic crust and it may be more available for dissolution due to hydrothermal processes compared to continental rocks. As a result the flux of hafnium from the oceanic crust into seawater, relative to the continental flux, may be higher than for neodymium, making it more visible.

6.17.6 LONG-LIVED RADIOGENIC TRACERS AND ICE-SHEET DYNAMICS

The previous discussions focused on utilizing long-lived radioactive systems, either dissolved in seawater or in authigenic precipitates. Here we discuss its utility in silicate detritus or individual minerals in marine sediments to follow the history of northern hemisphere ice sheets during the last glacial period. This is merely one example of the powerful potential of radiogenic isotopes as provenance tracers wih paleoceanographic implication.

Ice rafting was an important depositional process in the North Atlantic during Pleistocene glacial cycles (e.g., Ruddiman, 1977). The variable geologic age and history of land covered by ice sheets allows the potential for understanding their growth and evolution from millions to hundreds of year timescales through tracking of their detritus into marine sediments. As a result, the distribution of ice rafted detritus in the North Atlantic has been used to infer the major sources of icebergs and the general pattern of surface circulation. There has been a similar pattern of ice rafted deposition during glacial and interglacial times, with a southward shift in the locus of melting related to colder surface water in glacial times. Detailed studies of ice rafting in conjunction with other evidence for changes in the ocean–atmosphere–ice system in the North Atlantic provide important insights into processes that control climate conditions. A key element for understanding ocean–ice sheet–atmosphere interactions is identifying the major sources of ice-rafted detritus. In the following sections we give some examples of the application of isotopic provenance studies to constrain ice-rafted detritus (and thus iceberg) sources in the North Atlantic region.

6.17.6.1 Heinrich Events

"Heinrich events" of the North Atlantic are found as prominent layers, rich in ice-rafted detritus, within marine sediment cores (Heinrich, 1988). Heinrich layers are important as they may be related to extreme climate events worldwide (e.g. Broecker, 1994; Broecker and Hemming, 2001). The six Heinrich layers of the last glacial cycle can be divided into two groups based on the flux of ice-rafted grains and on the concentration of detrital carbonate in the coarse fraction (Bond *et al.*, 1992; Broecker *et al.*, 1992; Gwiazda *et al.*, 1996a; McManus *et al.*, 1998). Heinrich events are named in numerical order with H1 being the most recent. All six Heinrich layers are characterized by high percentages of ice-rafted detritus. However, in the case of H3 and H6 the flux of ice-rafted detritus, as indicated by number of lithic grains per gram or by $^{230}Th_{xs}$ measurements (McManus *et al.*, 1998), is not greatly increased relative to the background. Instead the high ice-rafted detritus percentage appears to be related to low foraminifera abundances. The array of data that have been collected on Heinrich layer provenance reveal a remarkably complete story of the geological history of the Heinrich layers' source. The four prominent Heinrich layers, H1, H2, H4, and H5, appear to have formed from massive discharges of icebergs from Hudson Strait. The provenance of these Heinrich layers is very distinctive within the IRD belt and hence can be mapped by any number of geochemical measurements. Isotopic studies to date have examined Heinrich layer provenance using K/Ar, Nd, Sr, and Pb isotopic techniques.

6.17.6.2 K/Ar ages of Heinrich Event Detritus

The first geochemical provenance measurement of the Heinrich layers was the K/Ar apparent age of <2 μm and 2–16 μm fine fractions (Jantschik and Huon, 1992). Ambient North Atlantic sediments have apparent K/Ar ages of ~400 Myr (Hurley *et al.*, 1963; Huon and Ruch, 1992; Jantschik and Huon, 1992), whereas the sediments from Heinrich layers H1, H2, H4, and H5 yielded apparent ages of ~1 Gyr. Variation in the potassium concentration is small, and thus the K/Ar age signal is a product of the radiogenic $^{40}Ar^{*}$ concentration (Hemming *et al.*, 2002a). Hemming *et al.* (2002a) showed that the $^{40}Ar^{*}$ is quite uniform in eastern North Atlantic cores and that the K/Ar age and $^{40}Ar/^{39}Ar$ spectra of <2 μm terrigenous sediment from Heinrich layer H2 in the eastern North Atlantic and from Orphan Knoll (southern Labrador Sea/western Atlantic) are indistinguishable. Taken together these results imply the entire fine fraction of Heinrich layer H2 was derived from sources bordering the Labrador Sea. The same pattern most likely characterizes H1, H4, and H5, because their K/Ar ages and $^{40}Ar^{*}$ concentrations are similar to H2 in eastern North Atlantic cores.

6.17.6.3 Nd–Sr–Pb Isotopes in Terrigenous Sediments

Strontium-isotope ratios are not particularly diagnostic of source terrain ages because Rb/Sr ratios are easily disturbed. However, Sm/Nd ratios tend to be conservative and neodymium-isotope ratios are effective tracers of the mean crustal age of sediment sources. Neodymium-isotope ratios of Heinrich layers H1, H2, H4, and H5 are consistent with derivation from a source with Archean heritage, and Grousset *et al.* (1993)

suggested sources surrounding the Labrador Sea or Baffin Bay (Figure 18). Strontium isotopes can be useful, however, when coupled with neodymium isotopes to trace the combined Sr–Nd characteristics of source terrains. Neodymium- and strontium-isotope ratios for different grain-size fractions from North Atlantic sediments suggest that the total terrigenous sediment load within these Heinrich layers in the IRD belt may be derived from the same limited range of sources (Revel *et al.*, 1996; Hemming *et al.*, 1998; Snoeckx *et al.*, 1999; Grousset *et al.*, 2000, 2001). The University of Colorado group has extensively characterized the composition of potential source areas in the vicinity of the Hudson Strait, Baffin Bay, other regions along the western Labrador coast, and the Gulf of St. Lawrence (Barber, 2001; Farmer *et al.*, 2003). Their data are consistent with a Hudson Strait provenance for Heinrich layers H1, H2, H4, and H5, and demonstrate an absence of substantial southeastern Laurentide ice sheet sources within pure Heinrich intervals. Lead-isotope ratios of the fine terrigenous fraction of Heinrich layers are distinctive (Hemming *et al.*, 1998), and are also consistent with derivation from the Hudson Strait region. New results from Farmer *et al.* (2003) may allow further distinction of fine-grained sediment sources with lead isotopes.

6.17.6.4 Isotopic and Geochronologic Measurements on Individual Mineral Grains

In addition to the bulk geochemical methods, several studies have examined individual grains or composite samples of feldspar grains for their lead-isotope ratios (Gwiazda *et al.*, 1996a,b; Hemming *et al.*, 1998), or individual grains of hornblende for their $^{40}Ar/^{39}Ar$ ages (Gwiazda *et al.*, 1996c; Hemming *et al.*, 1998, 2000b; Hemming and Hajdas, 2003). These studies provide remarkable insights into the geologic history of Heinrich layers that allow further refinement of the interpretations based on bulk isotopic analyses. Feldspars have high lead abundance and very low uranium and thorium abundance and thus the lead-isotope ratios of feldspar approximate the initial lead-isotope ratios of its source (e.g. Hemming *et al.*, 1994, 1996, 2000b). Lead-isotope data from Heinrich layer H1, H2, H4, and H5 feldspar grains form a linear trend that indicates an Archean (~2.7 Ga)

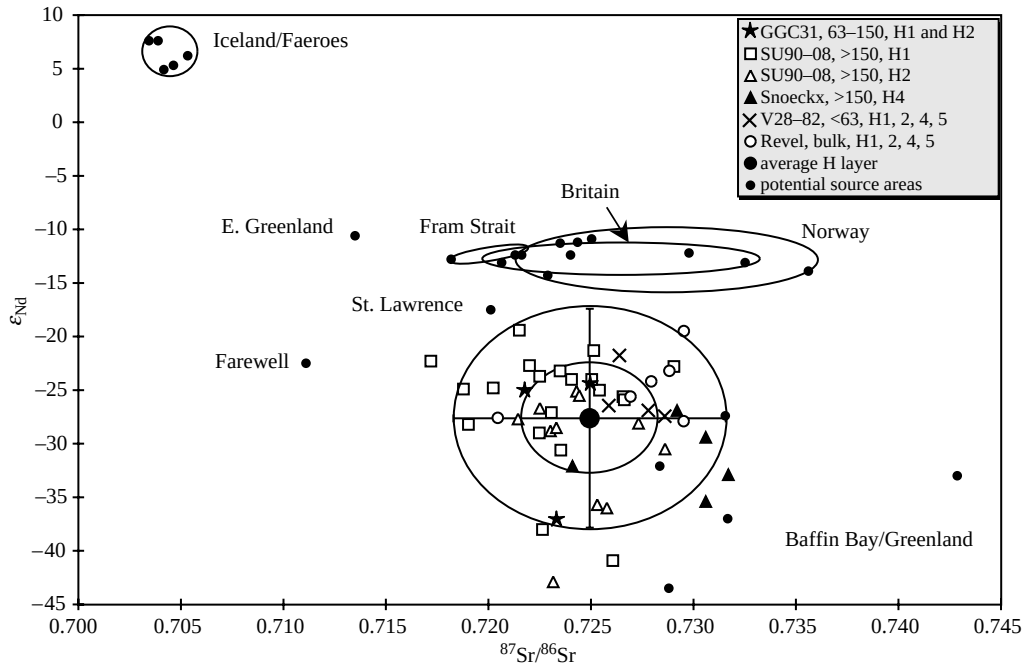

Figure 18 *Nd–Sr-isotope ratios of terrigenous clastic components of Heinrich layers H1, H2, H4, and H5.* Shown for reference are the average and 1 and 2 sigma range for the data published on these Heinrich layers and reported compositions of potential source areas of ice rafted detritus (Grousset *et al.*, 2001, and references therein). Note that the data are from different size fractions in different publications, but there is not evidence that there is a substantial bias even in the $^{87}Sr/^{86}Sr$ where one might be expected. This is most likely due to the large fraction of glacial flour with approximately the same composition in the fine as the coarse fraction in contrast to the way most sedimentary grain size variations are produced (Sources Grousset *et al.*, 2001; Snoeck *et al.*, 1999; Hemming *et al.*, 1998; Hemming, unpublished; Revel *et al.*, 1996).

heritage and a Paleoproterozoic (~1.8 Ga) metamorphic event (Figure 19(b)). Heinrich layer grains are similar in composition to H2 from Hudson Strait-proximal core HU87-009 and to feldspar grains from Baffin Island till (Hemming *et al.*, 2000b). However, they are distinctly different from feldspar grains from Gulf of St. Lawrence core V17-203, where Appalachian (Paleozoic) and Grenville (~1 Ga) sources are found. $^{40}Ar/^{39}Ar$ ages of individual hornblende grains from Heinrich layers H1, H2, H4, and H5 cluster around the implied Paleoproterozoic metamorphic events from the feldspar lead-isotope data (Gwiazda *et al.*, 1996c; Hemming *et al.*, 1998, 2000a; Hemming and Hajdas, 2003), and consistent with hornblende grains from Baffin Island tills (Hemming *et al.*, 2000b).

6.17.6.5 Contrasting Provenance of H3 and H6

Events H3 and H6 do not appear to be derived from the same sources as H1, H2, H4, and H5 (Figures 19(c) and 20). Using lead-isotope compositions of composite feldspar samples, Gwiazda *et al.* (1996a) found that H3 and H6 resemble the ambient sediment in V28-82, suggesting a large European source contribution, which agrees with the conclusion of Grousset *et al.* (1993). Lead-isotope data from composites of 75 to 300 grains from Gwiazda *et al.* (1996a) are shown in Figure 19(c). As mentioned above, H3 and H6 seem to be low-foraminifera intervals rather than ice-rafting events. These conclusions are consistent with other observations around the North Atlantic. Although Heinrich layer H3 appears to be a Hudson Strait event (Grousset *et al.*, 1993; Bond and Lotti, 1995; Rashid *et al.*, 2003, and Hemming, unpublished lead-isotope and $^{40}Ar/^{39}Ar$ hornblende data from Orphan Knoll), it does not spread Hudson Strait-derived IRD as far to the east as the other Heinrich events (Grousset *et al.*, 1993; Figure 19). Additionally, Kirby and Andrews (1999) proposed that H3 (and the Younger Dryas) represent across Strait (also modeled by Pfeffer *et al.*, 1997) rather than along Strait flow as inferred for H1, H2, H4, and H5. The strontium-isotope map of H3 shows a striking pattern of decrease in $^{87}Sr/^{86}Sr$ ratios nearly perpendicular to the IRD belt (Figure 21), consistent with a mixture of sediments from the Labrador Sea icebergs with those derived from icebergs from eastern Greenland, Iceland, and Europe. H6 has not been studied, but the composition of organic material in H3 does not stand out prominently in the studies mentioned above (Madureira *et al.*, 1997; Rosell-Mele *et al.*, 1997; Huon *et al.*, 2002).

6.17.6.6 Summary of Geochemical Provenance Analysis of Heinrich Layers

Heinrich layers H1, H2, H4, and H5 have several distinctive characteristics that distinguish them from ambient IRD, and they are derived from a mix of provenance components that are all consistent with derivation from a small region near Hudson Strait. Heinrich layers H3 and H6 have different sources, at least in the eastern North Atlantic. Less is known about H6, but H3 appears to have a Hudson Strait source in the southern Labrador Sea and western Atlantic, consistent with a similar but weaker event compared to the big four. Important related questions are as follows: How many types (provenance, flux, etc.) of Heinrich layers are there? Are IRD events in previous glacial intervals akin to the six in the last glacial period?

6.17.6.7 Trough Mouth Fans as Archives of Major IRD Sources

Trough mouth fans are major glacial-marine sediment fans that form when ice streams occupied glacial troughs that extend to the shelf-slope boundary (e.g., Vorren and Laberg, 1997). They are a significant resource and archive for understanding the potential compositional characteristics of sediment-laden icebergs, because they contain source-specific detrital material in highly concentrated accumulations. An important consideration that emphasizes the value of this archive is the recognition that the debris flows mimic the tills in the source area and, therefore, also the composition of the IRD in the calving icebergs. Furthermore, most icebergs experience substantial melting close to the ice-sheet margin, and the sediments they carry tend to melt out before the iceberg has reached the open ocean (Syvitski *et al.*, 1996; Andrews, 2000). Sediments deposited on the trough mouth fans are not only good representative point sources of the glacial drainage area; they are also located in positions of high iceberg production, that increase the likelihood of an iceberg's being carried to deep-marine environments in the surface-ocean currents before loosing its sediment load. Locations of documented trough mouth fans in the northern hemisphere are shown in Figure 22.

Although there is substantial overlap in the geological histories of the continental sources around the North Atlantic, there are also some systematic variations that can allow distinction of different sources. Realization of the full potential awaits characterizing the sources with multiple tracers as well as sedimentological studies, and documenting the geographic pattern of dispersal in marine sediments within small time-windows.

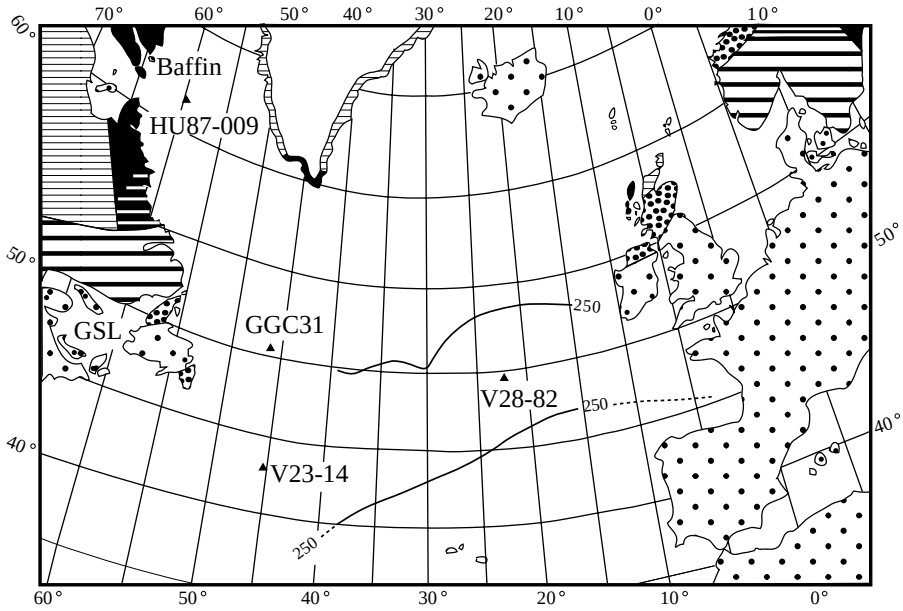
70°
60°
50°
40°
30°
20°
10°
0°
10°
60°
50°
40°
Baffin
HU87-009
GSL
GGC31
V28-82
V23-14
250
250
250

(a)

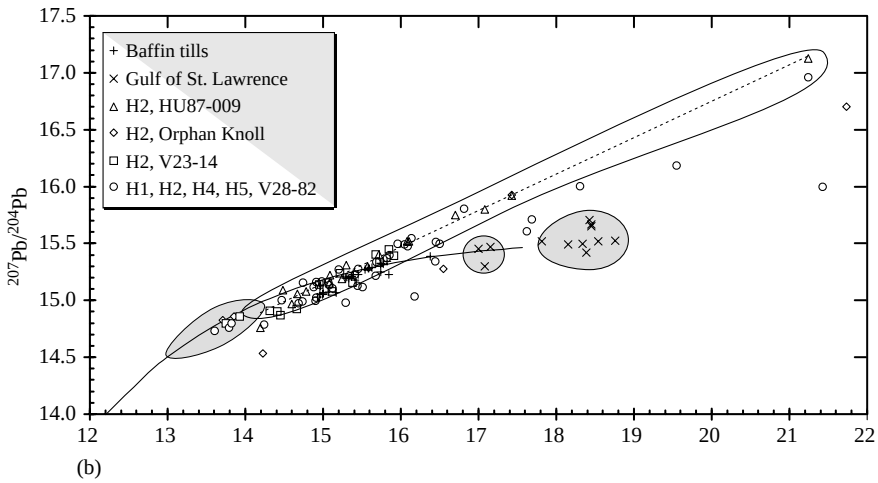
Baffin tills
Gulf of St. Lawrence
H2, HU87-009
H2, Orphan Knoll
H2, V23-14
H1, H2, H4, H5, V28-82
207Pb/204Pb
17.5
17.0
16.5
16.0
15.5
15.0
14.5
14.0
12
13
14
15
16
17
18
19
20
21
22

(b)

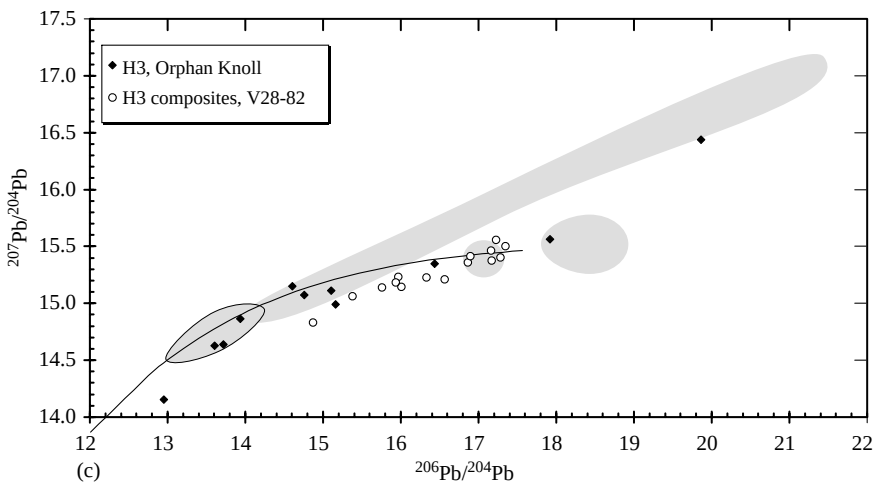
H3, Orphan Knoll
H3 composites, V28-82
207Pb/204Pb
17.5
17.0
16.5
16.0
15.5
15.0
14.5
14.0
12
13
14
15
16
17
18
19
20
21
22
206Pb/204Pb

(c)

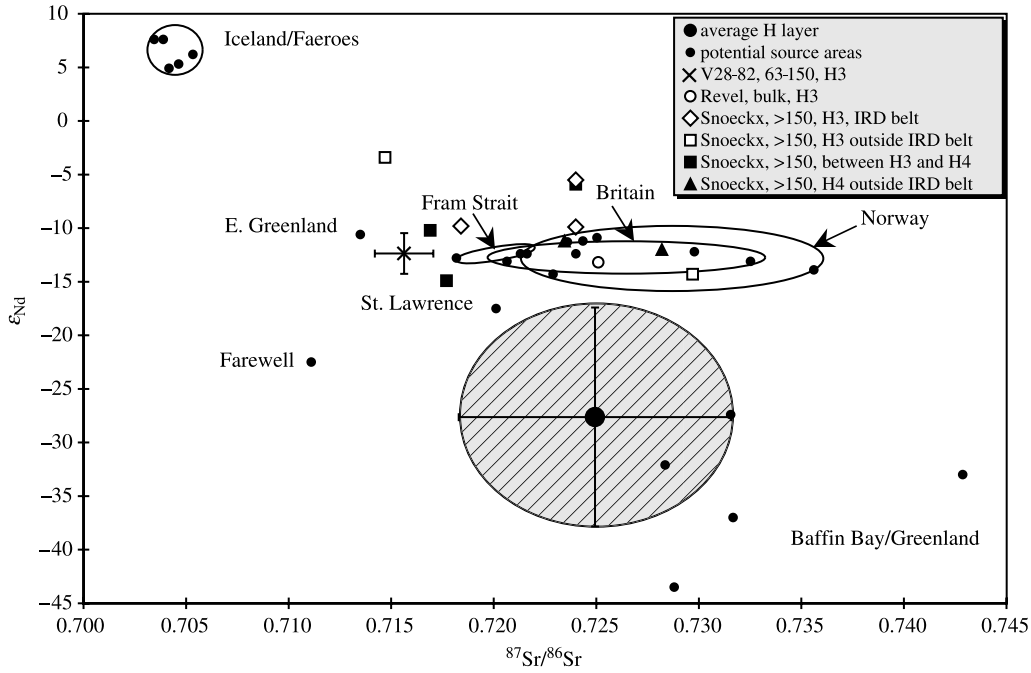

Figure 20 *Nd–Sr-isotope ratios of terrigenous clastic components of Heinrich layer H3.* Shown for reference are the average and 2 sigma range for the data published on Heinrich layers H1, H2, H4, and H5, and reported compositions of potential source areas of ice rafted detritus (Grousset *et al*., 2001, and references therein). Also included is the average of 5 unpublished analyses across H3 from V28-82, where the error bars represent the range of values measured (A. Jost and S. Hemming) (sources Grousset *et al*., 1993; Revel *et al*., 1996; Snoeckx *et al*., 1999).

A first step towards the goal of characterizing IRD sources in trough mouth fans was made by Hemming *et al*. (2002b) using $^{40}Ar/^{39}Ar$ data from populations of individual hornblende grains. The results conform closely to expectations based on the mapped ages of rocks in the region of the grains analyzed. For example, samples from the mid-Norwegian margin and from the northeastern margin of Greenland provide Caledonian ages. Samples from the Bear Island trough mouth fan have little hornblende indicating a dominant sedimentary source, and the hornblendes that are found yield a dominantly Paleoproterozoic spectrum of ages. Samples from near the southern tip of Greenland exhibit a mixture of Paleoproterozoic and a distinctive ~1.2 Ga population that is inferred to have derived from the alkaline Gardar complex. Samples from the Gulf of St. Lawrence have a virtually pure Grenville population, and samples from the Hudson Strait have a dominant Paleoproterozoic population with a small Archean contribution.

6.17.6.8 $^{40}Ar/^{39}Ar$ Hornblende Evidence for History of the Laurentide Ice Sheet During the Last Glacial Cycle

The history of the northern hemisphere ice sheets is an important aspect of the paleoclimate system. The layered record of IRD and other climate indicators preserved in deepsea sediment cores provides the potential to unravel the sequences of events surrounding important intervals during the last glacial cycle. Results of an extensive campaign to analyze the $^{40}Ar/^{39}Ar$ ages of multiple individual hornblende grains in core

Figure 19 *Pb isotopes in feldspar grains from Heinrich layers.* (a) Map showing locations of cores analyzed with geology and IRD belt for reference. (b) Data from Heinrich layers H1, H2, H4, and H5 from several North Atlantic and Labrador Sea cores. Also shown are data from Gulf of St. Lawrence core V17-203 (Hemming, unpublished data) and from Baffin Island tills (Hemming *et al*., 2002b). Reference fields are Superior province (Gariépy and Alle(c)gre, 1985), Labrador Sea reference line (LSRL, Gwiazda *et al*., 1996b), Grenville (DeWolf and Mezger, 1994) and Appalachian (Ayuso and Bevier, 1991). Data sources are H2 from HU87-009, V23-14, and V28-82 (Gwiazda *et al*., 1996b), Orphan Knoll core GGC31 (Hemming, unpublished), H1, H4, and H5 from V28-82 (Hemming *et al*., 1998). (c) Data from Heinrich layer H3 with reference fields from (b). Data sources are H3 from V28-82 (Gwiazda *et al*., 1996a), H3 from Orphan Knoll core GGC31 (Hemming, unpublished data).

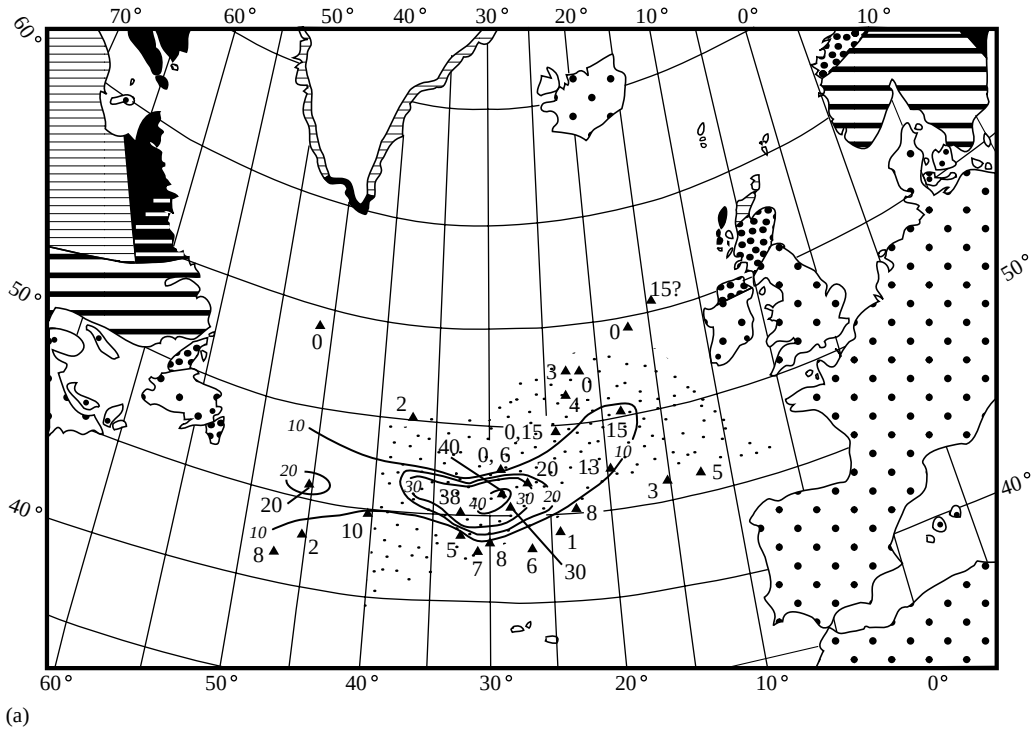

(a)

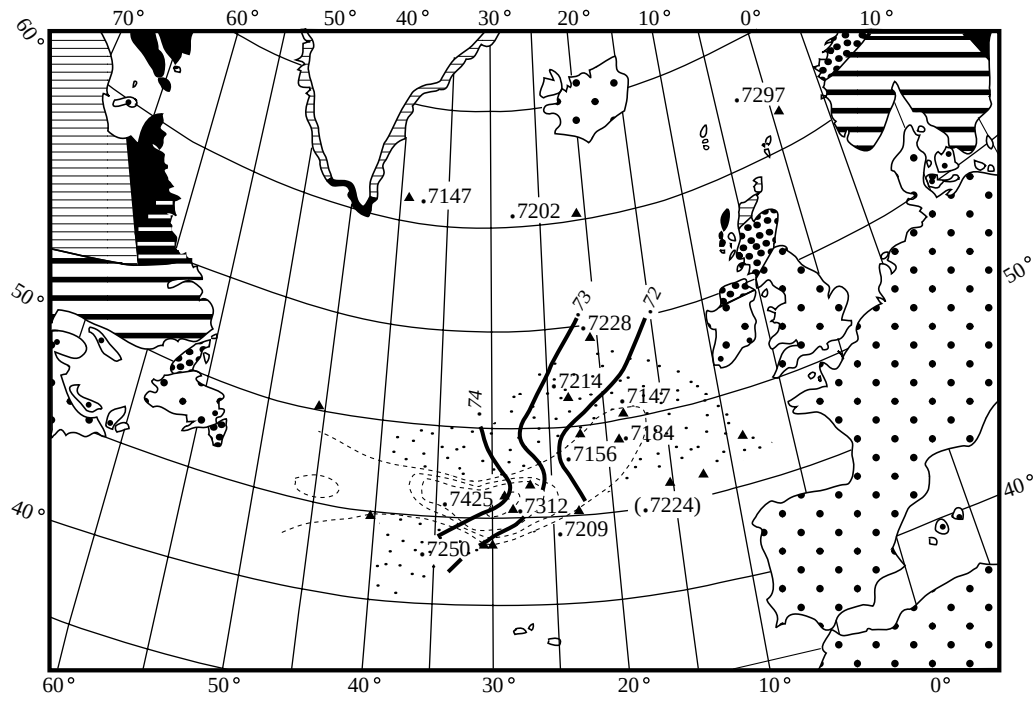

(b)

Figure 21 *Maps of data from Heinrich layer H3.* General geology and the Ruddiman (1977) IRD belt are shown. (a) Isopach map with 10 cm contour interval. (b) $^{87}Sr/^{86}Sr$ values for siliciclastic detritus in H3. Isopachs are shown in light dashed lines for reference. (c) 25–23 ka 250 mg cm^{-2} kyr^{-1} contours defining the approximately E–W IRD belt (Ruddiman, 1977), contours of 10, 50, and 100 sand-sized ash shards per cm^2 defining the approximately N–S trajectory of currents bringing Icelandic detritus into the North Atlantic (Ruddiman and Glover, 1982), and light dashed lines of 10 cm thickness intervals for H3.

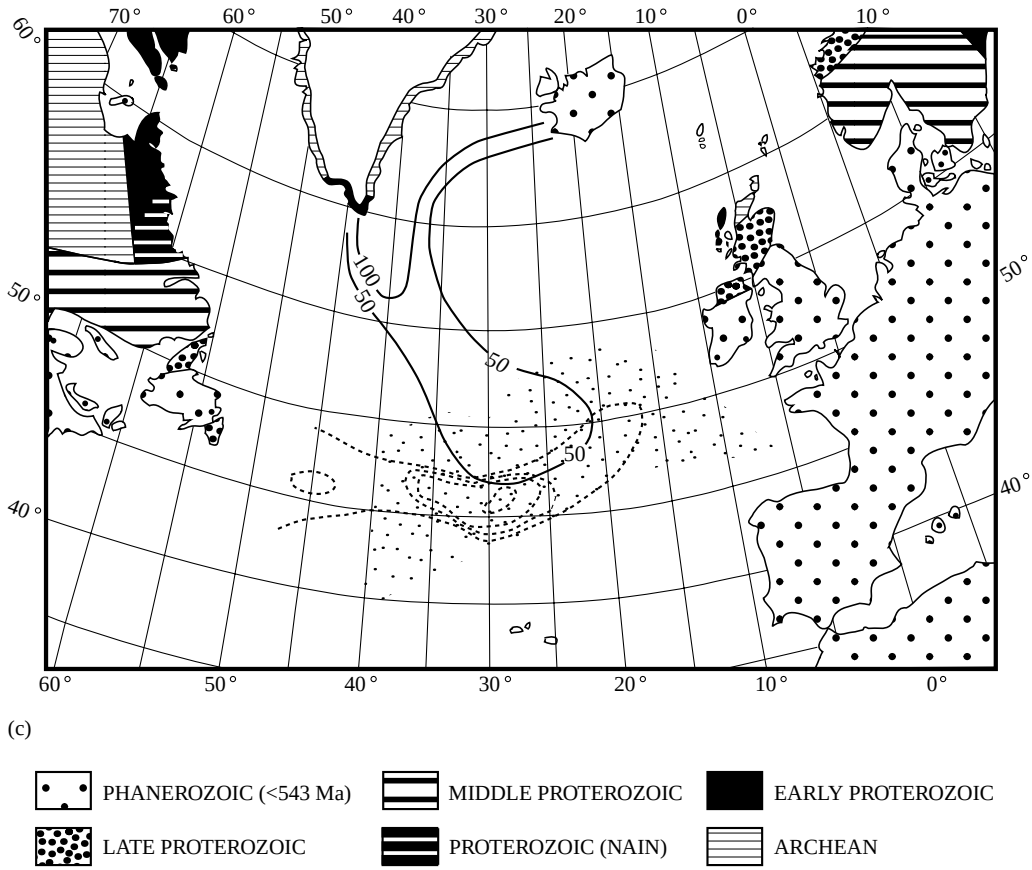

Figure 21 (continued).

V23-14 (Hemming and Hajdas, 2003) are presented as an example of the potential of this approach.

Core V23-14 is located within the thickest part of Ruddiman's (1977) ice-rafted detritus belt, and directly downstream of any Gulf of St. Lawrence region contributions (Figure 19(a)). Thus, the provenance of IRD from this core provides constraints on the evolution of the Laurentide ice sheet or smaller satellite ice sheets (e.g., Stea *et al*., 1998) and their iceberg contributions to the northwest Atlantic margin. The hornblende data are binned according to the age brackets based on known geological ages in the North Atlantic region. Data from within the Heinrich layers are lumped into one interval with an assumed duration of 0.1 kyr. There is some disagreement about the duration of Heinrich layers, ranging from estimates that they were virtually instantaneous, to estimates of 1,000 yr or more. Currently available published results of dating and flux methods used do not allow clearly constraining these estimates, although a best average estimate of duration is taken to be 500+/−250 yr. By lumping the Heinrich layer samples into a small interval, and plotting the cumulative fraction data against estimated age, we emphasize the ambient evolution of the Laurentide ice sheet (Figure 23).

In the period 42.5–26 ka (by ^{14}C dating), there is little evidence of iceberg contributions from Laurentian sources south of 55° N, which should provide dominantly Grenville and Appalachian ages. In contrast, in the period 26–14 ^{14}C ka, there is abundant evidence of contributions from this sector. Finally, in the period 14–6 ^{14}C ka, Grenville and Appalachian ages are again absent. These observations are consistent with the results of Hemming *et al*. (2000b) from Orphan Knoll in the interval above H2. They are also consistent with the observations of Ruddiman (1977), who presented ice-rafted detritus fluxes across the North Atlantic in several time intervals, including 40–25 ka, and 25–13 ka. The average flux appears to be approximately double the 40–25 ka flux in the 25–13 ka interval, and there is an overall correspondence between the flux of ice-rafted detritus and the extent of the northern hemisphere ice sheets (Ruddiman, 1977).

Results from studies of the ice-rafted detritus population from core V23-14 provide insights into the evolution of ice sheets of the northwest Atlantic margin since 43 ka. Between Heinrich layers H5 and H3 (MIS 3), it appears that the

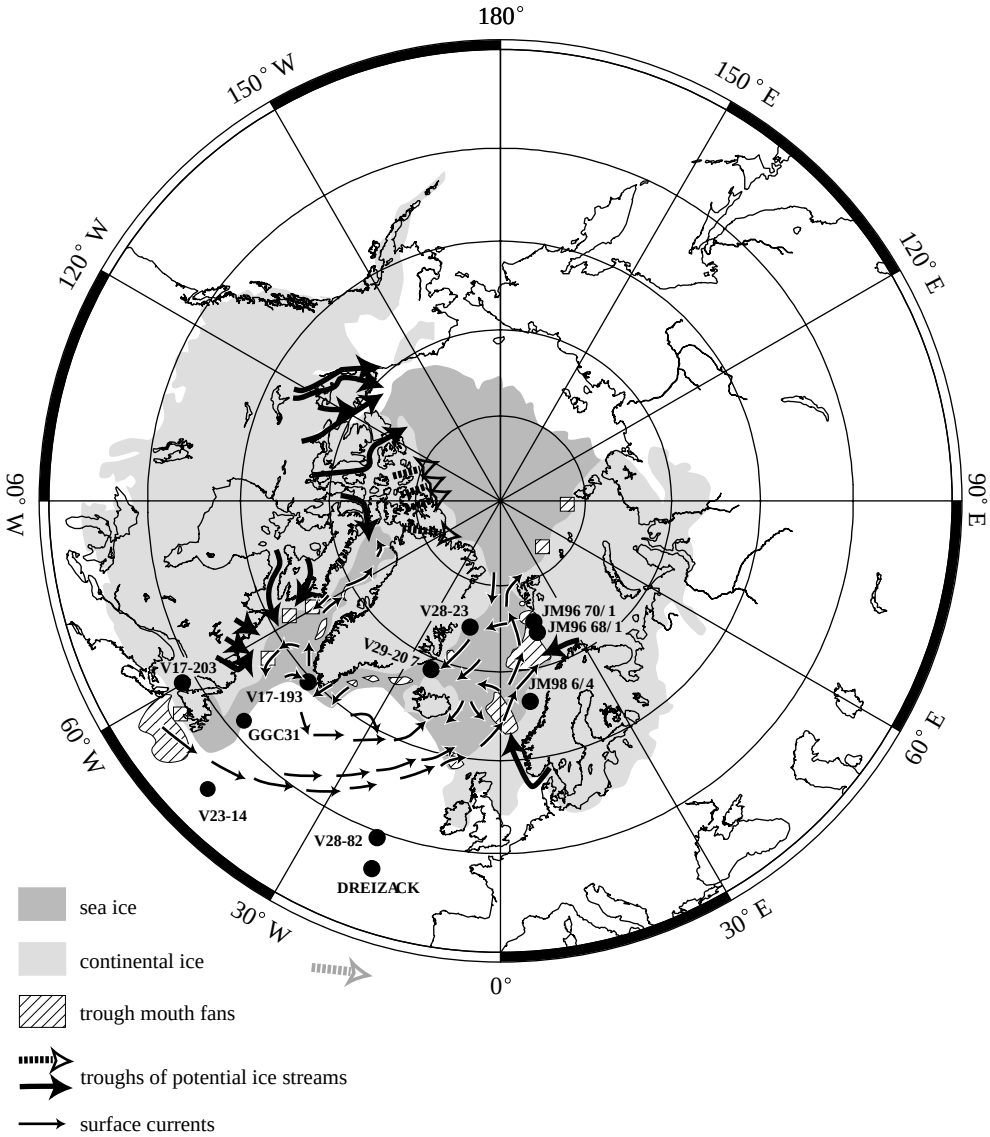

Figure 22 Polar projection from 40° to 90° showing the extents of continental and sea ice in the northern hemisphere, and cores presented and/or discussed here. The locations of known trough mouth fans are shown as well as inferred ice streams of the Laurentide ice sheet. Trough mouth fans (TMF) of the Nordic Seas are from Vorren and Laberg (1997), those around Greenland are from Funder *et al.* (1989), and along the western Labrador Sea are from Hesse and Khodabakhsh (1998). Arrows marking troughs across the Laurentide margin are based on mapping of J. Kleman. Arrow marking large trough feeding the North Sea TMF and the Barents Sea arrow indicating a large trough feeding Bear Island TMF is from Stokes and Clark (2001).

ice sheet (or sheets) did not extend far enough southeast to drop iceberg deposits with Grenville or Appalachian derivation into the North Atlantic. Between H3 and H1 (MIS 2), and outside the Heinrich layers, significant portions of the hornblende grains have ages indicating derivation from the southeastern sector, and thus indicate a significant expansion of the sheets at ~26 ^{14}C ka. After H1 (MIS 1), no detritus attributable to the southeastern sector is found, and judging from the present day situation, most of the ice-rafted detritus was likely derived from the Greenland ice sheet in the Holocene interval.

6.17.7 FINAL THOUGHTS

This chapter has summarized the basis for the application of long-lived isotopic tracers in oceanography and paleoceanography, focusing on neodymium isotopes in the oceans. It also summarized the current state of knowledge on the applications of these tracers to delineate the

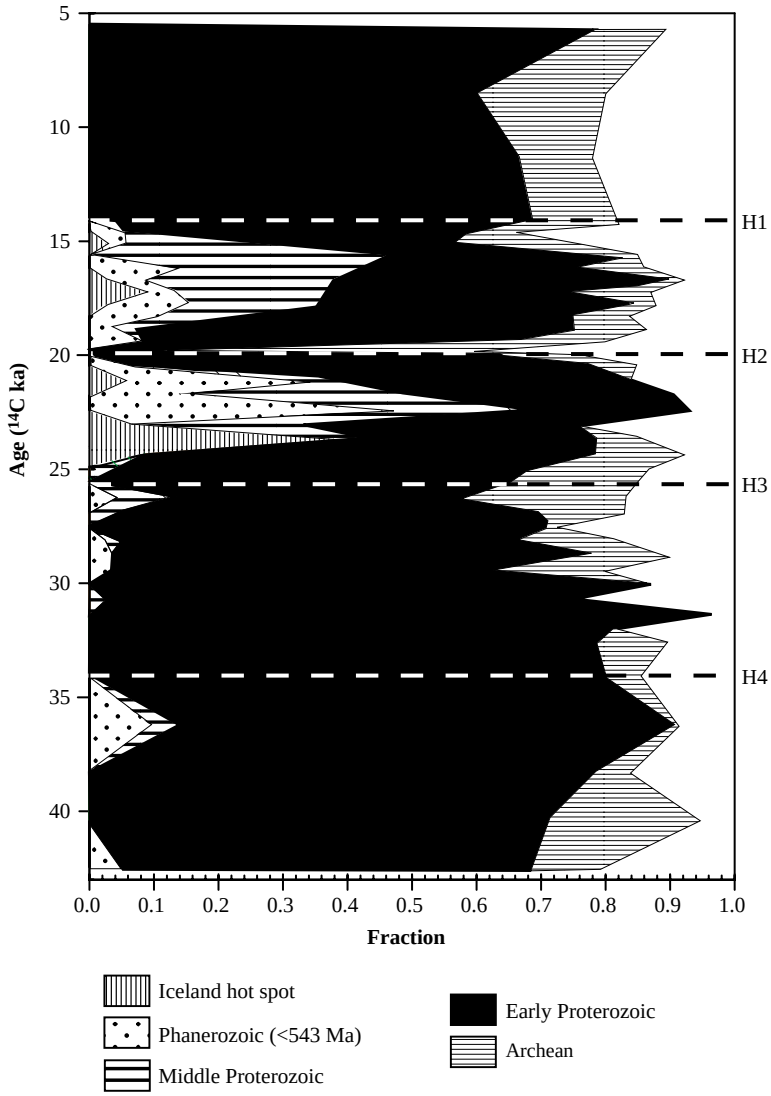

Figure 23 *Down-core plot of the hornblende Ar age populations from core V23-14*. Heinrich layers are indicated by the dashed lines (Source Hemming and Hajdas, 2003).

ice-sheet sources of North Atlantic Heinrich events. Especially since the early 1990s in particular, long-lived isotopic tracers have matured as paleoclimatic tools, as their potential value is becoming increasingly recognized and used by an growing number of investigators. Over the next decade they are certain to be among the primary methods used to generate new discoveries about the Earth's climatic history.

ACKNOWLEDGMENTS

This chapter is dedicated to Professors Gerald J. Wasserburg of Caltech, whose retirement roughly coincides with the publication of the Treatise, and Wally Broecker of LDEO. Gerry and colleagues characterized against all odds the neodymium isotopic variations in the global oceans, and the resulting body of work forms the basis of subsequent studies. Throughout his career Wally has greatly advanced the field of paleoceanography and global climate change, and has embraced the application of radiogenic isotope tracers. His contribution to emphasizing the importance of Heinrich layers is particularly relevant to this chapter. This is LDEO Contribution #6498.

REFERENCES

Abouchami W. and Goldstein S. L. (1995) A lead isotopic study of circum-antarctic manganese nodules. *Geochim. Cosmochim. Acta* **59**(9), 1809–1820.

Abouchami W., Goldstein S. L., Galer S. J. G., Eisenhauer A., and Mangini A. (1997) Secular changes of lead and

neodymium in central Pacific seawater recorded by a Fe–Mn crust. *Geochim. Cosmochim. Acta* **61**(18), 3957–3974.

Albare(c)de F. and Goldstein S. L. (1992) World map of Nd isotopes in sea-floor ferromanganese deposits. *Geology* **20**(8), 761–763.

Albare(c)de F., Goldstein S. L., and Dautel D. (1997) The neodymium isotopic composition of manganese nodules from the southern and Indian oceans, the global oceanic neodymium budget, and their bearing on deep ocean circulation. *Geochim. Cosmochim. Acta* **61**(6), 1277–1291.

Albare(c)de F., Simonetti A., Vervoort J. D., Blichert-Toft J., and Abouchami W. (1998) A Hf–Nd isotopic correlation in ferromanganese nodules. *Geophys. Res. Lett.* **25**(20), 3895–3898.

Amakawa H., Alibo D. S., and Nozaki Y. (2000) Nd isotopic composition and REE pattern in the surface waters of the eastern Indian Ocean and its adjacent seas. *Geochim. Cosmochim. Acta* **64**(10), 1715–1727.

Andrews J. T. (2000) Icebergs and iceerg rafted detritus (IRD) in the North Atlantic: facts and assumptions. *Oceanography* **13**, 100–108.

Ayuso R. A. and Bevier M. L. (1991) Regional differences in Pb isotopic compositions of feldspars in plutonic rocks of the northern appalachian mountains, USA and Canada: a geochrmical method of terrane correlation. *Tectonics* **10**, 191–212.

Balistrieri L., Brewer P. G., and Murray J. W. (1981) Scavenging residence times of trace-metals and surface-chemistry of sinking particles in the deep ocean. *Deep-sea Res. Part A: Oceanogr. Res. Pap.* **28**(2), 101–121.

Barber D. (2001) Laurentide ice sheet dynamics from 35 to 7 ka: Sr–Nd–Pb isotopic provenance of northwest Atlantic margin sediments. PhD, University of Colorado.

Bertram C. J. and Elderfield H. (1993) The geochemical balance of the rare-earth elements and neodymium isotopes in the oceans. *Geochim. Cosmochim. Acta* **57**(9), 1957–1986.

Bizzarro M., Baker J. A., Haack H., Ulfbeck D., and Rosing M. (2003) Early history of Earth's crust–mantle system inferred from hafnium isotopes in chondrites. *Nature* **421**(6926), 931–933.

Blichert-Toft J. and Albare(c)de F. (1997) The Lu–Hf isotope geochemistry of chondrites and the evolution of the mantle–crust system. *Earth Planet. Sci. Lett.* **148**(1–2), 243–258.

Bond G., Heinrich H., Broecker W., Labeyrie L., McManus J., Andrews J., Huon S., Jantschik R., Clasen S., Simet C., Tedesco K., Klas M., Bonani G., and Ivy S. (1992) Evidence for massive discharges of icebergs into the North-Atlantic Ocean during the last glacial period. *Nature* **360**(6401), 245–249.

Bond G. C. and Lotti R. (1995) Iceberg discharges into the North-Atlantic on millennial time scales during the last glaciation. *Science* **267**(5200), 1005–1010.

Bouquillon A., France-Lanord C., Michard A., and Tiercelin J. J. (1990) Sedimentology and isotopic chemistry of the Bengal fan sediments: the denudation of the Himalaya. *Proc. ODP Sci. Res.* **116**, 43–53.

Broecker W. S. (1994) Massive iceberg discharges as triggers for global climate-change. *Nature* **372**(6505), 421–424.

Broecker W. S. and Denton G. H. (1989) The role of ocean-atmosphere reorganizations in glacial cycles. *Geochim. Cosmochim. Acta* **53**, 2465–2501.

Broecker W. S. and Hemming S. (2001) Paleoclimate-climate swings come into focus. *Science* **294**(5550), 2308–2309.

Broecker W. S. and Peng T.-H. (1982) *Tracers in the Sea*. Eldigio Press, Palisades, NY.

Broecker W. S., Bond G. C., Klas M., Clark E., and McManus J. (1992) Origin of the Northern Atlantic's Heinrich events. *Clim. Dyn.* **6**, 265–293.

Burton K. W., Lee D. C., Christensen J. N., Halliday A. N., and Hein J. R. (1999) Actual timing of neodymium isotopic variations recorded by Fe–Mn crusts in the western North Atlantic. *Earth Planet. Sci. Lett.* **171**(1), 149–156.

Cantrell K. J. and Byrne R. H. (1987) Rare earth element complexation by carbonate and oxalate ions. *Geochim. Cosmochim. Acta* **51**, 597–605.

Charles C. D. and Fairbanks R. G. (1992) Evidence from Southern Ocean sediments for the effect of North Atlantic deep-water flux on climate. *Nature* **355**, 416–419.

Charles C. D., Lynch-Stieglitz J., Ninnemann U. S., and Fairbanks R. G. (1996) Climate connections between the hemisphere revealed by deep-sea sediment core/ice core correlations. *Earth Planet. Sci. Lett.* **142**, 19–27.

Chow T. J. and Patterson C. C. (1959) Lead isotopes in manganese nodules. *Geochim. Cosmochim. Acta* **17**, 21–31.

Chow T. J. and Patterson C. C. (1962) The occurence and significance of lead isotopes in pelagic sediments. *Geochim. Cosmochim. Acta* **26**, 263–308.

Dasch E. J., Dymond J. R., and Heath G. R. (1971) Isotopic analysis of metalliferous sediment from the east Pacific rise. *Earth Planet. Sci. Lett.* **13**, 175–180.

David K., Frank M., O'Nions R. K., Belshaw N. S., and Arden J. W. (2001) The Hf isotope composition of global seawater and the evolution of Hf isotopes in the deep Pacific Ocean from Fe–Mn crusts. *Chem. Geol.* **178**(1–4), 23–42.

Debaar H. J. W., Bacon M. P., and Brewer P. G. (1983) Rare-earth distributions with a positive Ce anomaly in the western North-Atlantic Ocean. *Nature* **301**(5898), 324–327.

Debaar H. J. W., Bacon M. P., Brewer P. G., and Bruland K. W. (1985) Rare-earth elements in the Pacific and Atlantic oceans. *Geochim. Cosmochim. Acta* **49**(9), 1943–1959.

DePaolo D. J. and Wasserburg G. J. (1976a) Nd isotopic variations and petrogenetic models. *Geophys. Res. Lett.* **3**, 249–252.

DePaolo D. J. and Wasserburg G. J. (1976b) Inferences about magma sources and mantle structure from variations of Nd-143–Nd-144. *Geophys. Res. Lett.* **3**(12), 743–746.

DeWolf C. P. and Mezger K. (1994) Lead isotope analyses of leached feldspars—constraints on the early crustal history of the Grenville Orogen. *Geochim. Cosmochim. Acta* **58**(24), 5537–5550.

Elderfield H. (1988) The oceanic chemistry of the rare-earth elements. *Phil. Trans. Roy. Soc. London Ser. A: Math. Phys. Eng. Sci.* **325**(1583), 105–126.

Elderfield H. and Greaves M. J. (1982) The rare earth elements in seawater. *Nature* **296**, 214–219.

Elderfield H., Hawkesworth C. J., Greaves M. J., and Caalvert S. E. (1981) Rare-earth element geochemistry of oceanic ferromanganese nodules and associated sediments. *Geochim. Cosmochim. Acta* **45**, 513–528.

Farmer G. L., Barber D., and Andrews J. (2003) Provenance of late quaternary ice-proximal sediments in the North Atlantic: Nd, Sr, and Pb isotopic evidence. *Earth Planet. Sci. Lett.* **209**(1–2), 227–243.

Frank M. (2002) Radiogenic isotopes: tracers of past ocean circulation and erosional input. *Rev. Geophys.* **40**(1) article no. 1001.

Frank M., Whiteley N., Kasten S., Hein J. R., and O'Nions K. (2002) North Atlantic deep water export to the southern ocean over the past 14 Myr: evidence from Nd and Pb isotopes in ferromanganese crusts. *Paleoceanography* **17**(2) article no. 1002.

Funder S., Larsen H. C., and Fredskild B. (1989) Quaternary geology of the ice-free areas and adjacent shelves of Greenland. In *Quaternary Geology of Canada and Greenland: K-1* (ed. R. J. Fulten). Geological Survey of Canada, Boulder, CO, pp. 741–792.

Galy A., FranceLanord C., and Derry L. A. (1996) The Late Oligocene Early Miocene Himalayan belt: constraints deduced from isotopic compositions of Early Miocene turbidites in the Bengal fan. *Tectonophysics* **260**(1–3), 109–118.

Gao S., Luo T. C., Zhang B. R., Zhang H. F., Han Y. W., Zhao Z. D., and Hu Y. K. (1998) Chemical composition of the

continental crust as revealed by studies in East China. *Geochim. Cosmochim. Acta* **62**(11), 1959–1975.

Gariépy C. and Alle(c)gre C. J. (1985) The lead isotope geochemistry and geochronology of late-kinematic intrucives from the Abitibi Greenstone belt, and the implications for late Archaean crustal evolution. *Geochim. Cosmochim. Acta* **49**, 2371–2383.

Godfrey L. V., Lee D. C., Sangrey W. F., Halliday A. N., Salters V. J. M., Hein J. R., and White W. M. (1997) The Hf isotopic composition of ferromanganese nodules and crusts and hydrothermal manganese deposits: implications for seawater Hf. *Earth Planet. Sci. Lett.* **151**(1–2), 91–105.

Goldstein S. J. and Jacobsen S. B. (1988) Nd and Sr isotopic systematics of river water suspended material—implications for crustal evolution. *Earth Planet. Sci. Lett.* **87**(3), 249–265.

Goldstein S. L. and O'Nions R. K. (1981) Nd and Sr isotopic relationships in pelagic clays and ferromanganese deposits. *Nature* **292**, 324–327.

Goldstein S. L., Onions R. K., and Hamilton P. J. (1984) A Sm–Nd isotopic study of atmospheric dusts and particulates from major river systems. *Earth Planet. Sci. Lett.* **70**(2), 221–236.

Grousset F. E., Labeyrie L., Sinko J. A., Cremer M., Bond G., Duprat J., Cortijo E., and Huon S. (1993) Patterns of ice-rafted detritus in the glacial North-Atlantic (40-degrees-55-degrees-N). *Paleoceanography* **8**(2), 175–192.

Grousset F. E., Pujol C., Labeyrie L., Auffret G., and Boelaert A. (2000) Were the North Atlantic Heinrich events triggered by the behavior of the European ice sheets? *Geology* **28**(2), 123–126.

Grousset F. E., Cortijo E., Huon S., Herve L., Richter T., Burdloff D., Duprat J., and Weber O. (2001) Zooming in on Heinrich layers. *Paleoceanography* **16**(3), 240–259.

Gwiazda R. H., Hemming S. R., and Broecker W. S. (1996a) Provenance of icebergs during Heinrich event 3 and the contrast to their sources during other Heinrich episodes. *Paleoceanography* **11**(4), 371–378.

Gwiazda R. H., Hemming S. R., and Broecker W. S. (1996b) Tracking the sources of icebergs with lead isotopes: the provenance of ice-rafted debris in Heinrich layer 2. *Paleoceanography* **11**(1), 77–93.

Gwiazda R. H., Hemming S. R., Broecker W. S., Onsttot T., and Mueller C. (1996c) Evidence from Ar-40/Ar-39 ages for a Churchill province source of ice-rafted amphiboles in Heinrich layer 2. *J. Glaciol.* **42**(142), 440–446.

Heinrich H. (1988) Origin and consequences of cyclic ice rafting in the northeast Atlantic Ocean during the past 130, 000 years. *Quat. Res.* **29**(2), 142–152.

Hemming S. R. and Hajdas I. (2003) Ice-rafted detritus evidence from Ar-40/Ar-39 ages of individual hornblende grains for evolution of the eastern margin of the Laurentide ice sheet since 43 C-14 ky. *Quat. Int.* **99**, 29–43.

Hemming S. R., McLennan S. M., and Hanson G. N. (1994) Lead isotopes as a provenance tool for quartz—examples from Plutons and Quartzite, northeastern Minnesota, USA. *Geochim. Cosmochim. Acta* **58**(20), 4455–4464.

Hemming S. R., McDaniel D. K., McLennan S. M., and Hanson G. N. (1996) Pb isotope constraints on the provenance and diagenesis of detrital feldspars from the Sudbury basin, Canada. *Earth Planet. Sci. Lett.* **142**(3–4), 501–512.

Hemming S. R., Broecker W. S., Sharp W. D., Bond G. C., Gwiazda R. H., McManus J. F., Klas M., and Hajdas I. (1998) Provenance of Heinrich layers in core V28-82, northeastern Atlantic: Ar-40/Ar-39 ages of ice-rafted hornblende, Pb isotopes in feldspar grains, and Nd–Sr–Pb isotopes in the fine sediment fraction. *Earth Planet. Sci. Lett.* **164**(1–2), 317–333.

Hemming S. R., Bond G. C., Broecker W. S., Sharp W. D., and Klas-Mendelson M. (2000a) Evidence from 40Ar–39Ar ages of individual hornblende grains for varying Laurenide sources of iceberg discharges 22,000 to 10,500 yr BP. *Quat. Res.* **54**, 372–373.

Hemming S. R., Gwiazda R. H., Andrews J. T., Broecker W. S., Jennings A. E., and Onstott T. C. (2000b) Ar-40/Ar-39 and Pb–Pb study of individual hornblende and feldspar grains from southeastern Baffin Island glacial sediments: implications for the provenance of the Heinrich layers. *Can. J. Earth Sci.* **37**(6), 879–890.

Hemming S. R., Hall C. M., Biscaye P. E., Higgins S. M., Bond G. C., McManus J. F., Barber D. C., Andrews J. T., and Broecker W. S. (2002a) Ar-40/Ar-39 ages and Ar-40* concentrations of fine-grained sediment fractions from North Atlantic Heinrich layers. *Chem. Geol.* **182**(2–4), 583–603.

Hemming S. R., Vorren T. O., and Kleman J. (2002b) Provinciality of ice rafting in the North Atlantic: application of Ar-40/Ar-39 dating of individual ice rafted hornblende grains. *Quat. Int.* **95–96**, 75–85.

Henry F., Jeandel C., Dupre B., and Minster J. F. (1994) Particulate and dissolved Nd in the western Mediteranean Sea: sources, fate and budget. *Mar. Chem.* **45**, 283–305.

Hesse R. and Khodabakhsh S. (1998) Depositional facies of late Pleistocene Heinrich events in the Labrador Sea. *Geology* **26**(2), 103–106.

Hofmann A. W., Jochum K. P., Seufert M., and White W. M. (1986) Nb and Pb in oceanic basalts: new constraints on mantle evolution. *Earth Planet. Sci. Lett.* **79**, 33–45.

Huon S. and Ruch P. (1992) Mineralogical, K–Ar and Sr-87/Sr-86 isotope studies of Holocene and late glacial sediments in a deep-sea core from the northeast Atlantic Ocean. *Mar. Geol.* **107**(4), 275–282.

Huon S., Grousset F. E., Burdloff D., Bardoux G., and Mariotti A. (2002) Sources of fine-sized organic matter in North Atlantic Heinrich layers: delta C-13 and delta N-15 tracers. *Geochim. Cosmochim. Acta* **66**(2), 223–239.

Hurley P. M., Heezen B. C., Pinson W. H., and Fairbairn H. W. (1963) K–Ar values in pelagic sediments of the North Atlantic. *Geochim. Cosmochim. Acta* **27**, 393–399.

Jacobsen S. B. and Wasserburg G. J. (1980) Sm–Nd isotopic evolution of chondrites. *Earth Planet. Sci. Lett.* (50), 139–155.

Jaffey A. H., Flynn K. F., Glendeni Le., Bentley W. C., and Essling A. M. (1971) Precision measurement of half-lives and specific activities of U-235 and U-238. *Phys. Rev. C* **4**(5), 1889ff.

Jantschik R. and Huon S. (1992) Detrital silicates in Northeast Atlantic deep-sea sediments during the Late Quaternary—mineralogical and K–Ar isotopic data. *Eclogae Geologicae Helvetiae* **85**(1), 195–212.

Jeandel C. (1993) Concentration and isotopic composition of Nd in the South-Atlantic Ocean. *Earth Planet. Sci. Lett.* **117**(3–4), 581–591.

Jeandel C., Bishop J. K., and Zindler A. (1995) Exchange of neodymium and its isotopes between seawater and small and large particles in the Sargasso Sea. *Geochim. Cosmochim. Acta* **59**(3), 535–547.

Jeandel C., Thouron D., and Fieux M. (1998) Concentrations and isotopic compositions of neodymium in the eastern Indian Ocean and Indonesian straits. *Geochim. Cosmochim. Acta* **62**(15), 2597–2607.

Jones C. E., Halliday A. N., Rea D. K., and Owen R. M. (1994) Neodymium isotopic variations in North Pacific modern silicate sediment and the insignificance of detrital ree contributions to seawater. *Earth Planet. Sci. Lett.* **127**(1–4), 55–66.

Kirby M. E. and Andrews J. T. (1999) Mid-Wisconsin Laurentide ice sheet growth and decay: implications for Heinrich events 3 and 4. *Paleoceanography* **14**(2), 211–223.

Lacan F. and Jeandel C. (2001) Tracing Papua New Guinea imprint on the central Equatorial Pacific Ocean using neodymium isotopic compositions and rare earth element patterns. *Earth Planet. Sci. Lett.* **186**(3–4), 497–512.

Le Roux L. J. and Glendenin L. E. (1963) Half-life of ^{232}Th. *Proc. Natl. Meet. Nuclear Energy*, 83–94.

Levitus S. (1994) *World Ocean Atlas*. US Department of Commerce, Boulder, CO.

Lugmair G. and Scheinin N. B. (1974) Sm–Nd ages: a new dating method. *Meteoritics* **19**, 369.

Madureira L. A. S., vanKreveld S. A., Eglinton G., Conte M., Ganssen G., vanHinte J. E., and Ottens J. J. (1997) Late quaternary high-resolution biomarker and other sedimentary climate proxies in a northeast Atlantic core. *Paleoceanography* **12**(2), 255–269.

McManus J. F., Anderson R. F., Broecker W. S., Fleisher M. Q., and Higgins S. M. (1998) Radiometrically determined sedimentary fluxes in the sub-polar North Atlantic during the last 140,000 years. *Earth Planet. Sci. Lett.* **155**(1–2), 29–43.

Michard A., Albarede F., Michard G., Minster J. F., and Charlou J. L. (1983) Rare-earth elements and uranium in high-temperature solutions from East Pacific Rise hydrothermal vent field (13-degrees-N). *Nature* **303**(5920), 795–797.

Nakai S., Halliday A. N., and Rea D. K. (1993) Provenance of dust in the Pacific Ocean. *Earth Planet. Sci. Lett.* **119**(1–2), 143–157.

Neumann W. and Huster E. (1976) Discussion of Rb-87 half-life determined by absolute counting. *Earth Planet. Sci. Lett.* **33**(2), 277–288.

O'Nions R. K., Hamilton P. J., and Evensen N. M. (1977) Variations in ^{143}Nd/^{144}Nd and ^{87}Sr/^{86}Sr ratios in oceanic basalts. *Earth Planet. Sci. Lett.* **34**, 13–22.

O'Nions R. K., Carter S. R., Cohen R. S., Evensen N. M., and Hamilton P. J. (1978) Nd and Sr isotopes in oceanic ferromanganese deposits and ocean floor basalts. *Nature* **273**, 435–438.

Patchett P. J., White W. M., Feldmann H., Kielinczuk S., and Hofmann A. W. (1984) Hafnium rare-earth element fractionation in the sedimentary system and crustal recycling into the earths mantle. *Earth Planet. Sci. Lett.* **69**(2), 365–378.

Patterson C. C. (1956) The age of meteorites and the earth. *Geochim. Cosmochim. Acta* **10**, 230–237.

Patterson C. C., Goldberg E. D., and Inghram M. G. (1953) Isotopic compositions of quaternary leads from the Pacific Ocean. *Bull. Geol. Soc. Am.* **64**, 1387–1388.

Pfeffer W. T., Dyurgerov M., Kaplan M., Dwyer J., Sassolas C., Jennings A., Raup B., and Manley W. (1997) Numerical modeling of late Glacial Laurentide advance of ice across Hudson Strait: insights into terrestrial and marine geology, mass balance, and calving flux. *Paleoceanography* **12**(1), 97–110.

Piepgras D. J. and Jacobsen S. B. (1988) The isotopic composition of neodymium in the North Pacific. *Geochim. Cosmochim. Acta* **52**(6), 1373–1381.

Piepgras D. J. and Wasserburg G. J. (1980) Neodymium isotopic variations in seawater. *Earth Planet. Sci. Lett.* **50**, 128–138.

Piepgras D. J. and Wasserburg G. J. (1982) Isotopic composition of neodymium in waters from the Drake Passage. *Science* **217**(4556), 207–214.

Piepgras D. J. and Wasserburg G. J. (1983) Influence of the Mediterranean outflow on the isotopic composition of neodymium in waters of the North-Atlantic. *J. Geophys. Res.: Oceans Atmos.* **88**(NC10), 5997–6006.

Piepgras D. J. and Wasserburg G. J. (1985) Strontium and neodymium isotopes in hot springs on the East Pacific Rise and Guaymas Basin. *Earth Planet. Sci. Lett.* **72**(4), 341–356.

Piepgras D. J. and Wasserburg G. J. (1987) Rare-earth element transport in the western North-Atlantic inferred from Nd isotopic observations. *Geochim. Cosmochim. Acta* **51**(5), 1257–1271.

Piepgras D. J., Wasserburg G. J., and Dasch E. J. (1979) The isotopic composition of Nd in different ocean masses. *Earth Planet. Sci. Lett.* **45**, 223–236.

Pierson-Wickmann A. C., Reisberg L., France-Lanord C., and Kudrass H. R. (2001) Os–Sr–Nd results from sediments in the Bay of Bengal: implications for sediment transport and the marine Os record. *Paleoceanography* **16**(4), 435–444.

Piotrowski A. M., Lee D. C., Christensen J. N., Burton K. W., Halliday A. N., Hein J. R., and Gunther D. (2000) Changes in erosion and ocean circulation recorded in the Hf isotopic compositions of North Atlantic and Indian Ocean ferromanganese crusts. *Earth Planet. Sci. Lett.* **181**(3), 315–325.

Rashid H., Hesse R., and Piper D. J. W. (2003) Distribution, thickness and origin of Heinrich layer 3 in the Labrador Sea. *Earth Planet. Sci. Lett.* **205**(3–4), 281–293.

Revel M., Sinko J. A., Grousset F. E., and Biscaye P. E. (1996) Sr and Nd isotopes as tracers of North Atlantic lithic particles: paleoclimatic implications. *Paleoceanography* **11**(1), 95–113.

Reynolds P. H. and Dasch E. J. (1971) Lead isotopes in marine manganese nodules and the ore-lead growth curve. *J. Geophys. Res.* **76**, 5124–5129.

Richard P., Shimizu N., and Alle(c)gre C. J. (1976) ^{143}Nd/^{146}Nd, a natural tracer: an application to oceanic basalts. *Earth Planet. Sci. Lett.* **31**, 269–278.

Rintoul S. R. (1991) South Atlantic interbasin exchange. *J. Geophys. Res.* **96**, 2675–2692.

Rosell-Mele A., Maslin M. A., Maxwell J. R., and Schaeffer P. (1997) Biomarker evidence for "Heinrich" events. *Geochim. Cosmochim. Acta* **61**(8), 1671–1678.

Ruddiman W. F. (1977) Late quaternary deposition of ice-rafted sand in subpolar North-Atlantic (Lat 40-degrees to 65-degrees-N). *Geol. Soc. Am. Bull.* **88**(12), 1813–1827.

Ruddiman W. F. and Glover L. K. (1982) Mixing of volcanic ash zones in subpolar North Atlantic sediments. In *The Ocean Floor, Bruce C. Heezen Memorial Volume* (eds. R. A. Scrutton and M. Talwani). Wiley, Chichester, NY, pp. 37–60.

Rudnick R. L. and Fountain D. M. (1995) Nature and composition of the continental-crust—a lower crustal perspective. *Rev. Geophys.* **33**(3), 267–309.

Rutberg R. L., Hemming S. R., and Goldstein S. L. (2000) Reduced north Atlantic deep water flux to the glacial southern ocean inferred from neodymium isotope ratios. *Nature* **405**(6789), 935–938.

Scherer E., Munker C., and Mezger K. (2001) Calibration of the lutetium–hafnium clock. *Science* **293**(5530), 683–687.

Schlosser P., Bullister J. L., Fine R., Jenkim W. J., Key R., Lupton J., Roether W., and Smethie W. M. Jr. (2001) Transformation and age of water masses. In *Ocean circulation and climate: Observing and Modelling the Global Ocean* (eds G. Siedler, J. Church, and J. Gould). Academic Press, pp. 431–452.

Segl M., Mangini A., Bonani G., Hofmann H. J., Nessi M., Suter M., Wölfli W., Friedrich G., Plüger W. L., Wiechowski A., and Beer J. (1984) ^{10}Be-dating of a manganese crust from central North Pacific and implications for ocean palaeocirculation. *Nature* **309**, 540–543.

Sguigna A. P., Larabee A. J., and Waddington J. C. (1982) The half-life of Lu-176 by a gamma–gamma coincidence measurement. *Can. J. Phys.* **60**(3), 361–364.

Shimizu H., Tachikawa K., Masuda A., and Nozaki Y. (1994) Cerium and neodymium isotope ratios and ree patterns in seawater from the North Pacific Ocean. *Geochim. Cosmochim. Acta* **58**(1), 323–333.

Snoeckx H., Grousset F., Revel M., and Boelaert A. (1999) European contribution of ice-rafted sand to Heinrich layers H3 and H4. *Mar. Geol.* **158**(1–4), 197–208.

Spivack A. J. and Wasserburg G. J. (1988) Neodymium isotopic composition of the Mediterranean outflow and the eastern North-Atlantic. *Geochim. Cosmochim. Acta* **52**(12), 2767–2773.

Stea R. R., Piper D. J. W., Fader G. B. J., and Boyd R. (1998) Wisconsinan glacial and sea-level history of Maritime

Canada and the adjacent continental shelf: a correlation of land and sea events. *Geol. Soc. Am. Bull.* **110**(7), 821–845.

Steiger R. H. and Jäger E. (1977) Subcommission on geochronology—convention on use of decay constants in geochronology and cosmochronology. *Earth Planet. Sci. Lett.* **36**(3), 359–362.

Stokes C. R. and Clark C. D. (2001) Palaeo-ice streams. *Quat. Sci. Rev.* **20**(13), 1437–1457.

Stordal M. C. and Wasserburg G. J. (1986) Neodymium isotopic study of Baffin-bay water—sources of Ree from very old terranes. *Earth Planet. Sci. Lett.* **77**(3–4), 259–272.

Syvitski J. P. M., Andrews J. T., and Dowdeswell J. A. (1996) Sediment deposition in an iceberg-dominated glacimarine environment, East Greenland: basin fill implications. *Global Planet. Change* **12**(1–4), 251–270.

Tachikawa K., Jeandel C., and Dupre B. (1997) Distribution of rare earth elements and neodymium isotopes in settling particulate material of the tropical Atlantic Ocean (EUMELI site). *Deep-Sea Res. I: Oceanogr. Res. Pap.* **44**(11), 1769–1792.

Tachikawa K., Jeandel C., and Roy-Barman M. (1999a) A new approach to the Nd residence time in the ocean: the role of atmospheric inputs. *Earth Planet. Sci. Lett.* **170**(4), 433–446.

Tachikawa K., Jeandel C., Vangriesheim A., and Dupre B. (1999b) Distribution of rare earth elements and neodymium isotopes in suspended particles of the tropical Atlantic Ocean (EUMELI site). *Deep-Sea Res. I: Oceanogr. Res. Pap.* **46**(5), 733–755.

Tatsumoto M., Knight R. J., and Allegre C. J. (1973) Time differences in formation of meteorites as determined from ratio of Pb-207 to Pb-206. *Science* **180**(4092), 1279–1283.

Tatsumoto M., Unruh D. M., and Patchett P. J. (1981) U-Pb nd Lu–;Hf systematics of Antarctic meteorites. *Proc. 6th Symp. Antarctic Meteorit.*, 237–249.

Taylor S. R. and McLennan S. M. (1985) *The Continental Crust: Its Composition and Evolution*. Blackwell, Oxford.

van de Flierdt T., Frank M., Lee D. C., and Halliday A. N. (2002) Glacial weathering and the hafnium isotope composition of seawater. *Earth Planet. Sci. Lett.* **198**(1–2), 167–175.

Vance D. and Burton K. (1999) Neodymium isotopes in planktonic foraminifera: a record of the response of continental weathering and ocean circulation rates to climate change. *Earth Planet. Sci. Lett.* **173**(4), 365–379.

Vervoort J. D., Patchett P. J., Gehrels G. E., and Nutman A. P. (1996) Constraints on early Earth differentiation from hafnium and neodymium isotopes. *Nature* **379**(6566), 624–627.

Vervoort J. D., Patchett P. J., Blichert-Toft J., and Albarede F. (1999) Relationships between Lu–Hf and Sm–Nd isotopic systems in the global sedimentary system. *Earth Planet. Sci. Lett.* **168**(1–2), 79–99.

von Blanckenburg F. (1999) Perspectives: paleoceanography—tracing past ocean circulation? *Science* **286**(5446), 1862–1863.

von Blanckenburg F. and Nagler T. F. (2001) Weathering versus circulation-controlled changes in radiogenic isotope tracer composition of the Labrador Sea and North Atlantic deep water. *Paleoceanography* **16**(4), 424–434.

von Blanckenburg F., O'Nions R. K., and Hein J. R. (1996) Distribution and sources of pre-anthropogenic lead isotopes in deep ocean water from Fe–Mn crusts. *Geochim. Cosmochim. Acta* **60**(24), 4957–4963.

Vorren T. O. and Laberg J. S. (1997) Trough mouth fans—Palaeoclimate and ice-sheet monitors. *Quat. Sci. Rev.* **16**(8), 865–881.

Wedepohl K. H. (1995) The composition of the continental-crust. *Geochim. Cosmochim. Acta* **59**(7), 1217–1232.

White W. M., Patchett J., and Ben Othman D. (1986) Hf isotope ratios of marine sediments and Mn nodules: evidence for a mantle source of Hf in seawater. *Earth Planet. Sci. Lett.* **79**, 46–54.

Treatise on Geochemistry
ISBN (set): 0-08-043751-6
Volume 6; (ISBN: 0-08-044341-9); pp. 453–489